ACS central science

http://pubs.acs.org/journal/acscii

Research Article

Elevated Vacuolar Uptake of Fluorescently Labeled Antifungal Drug Caspofungin Predicts Echinocandin Resistance in Pathogenic Yeast

Qais Z. Jaber, Maayan Bibi, Ewa Ksiezopolska, Toni Gabaldon, Judith Berman,* and Micha Fridman*

Cite This: *ACS Cent. Sci.* 2020, 6, 1698–1712

Read Online

ACCESS | Metrics & More | Article Recommendations | Supporting Information

ABSTRACT: Echinocandins are the newest class of antifungal drugs in clinical use. These agents inhibit β-glucan synthase, which catalyzes the synthesis of β-glucan, an essential component of the fungal cell wall, and have a high clinical efficacy and low toxicity. Echinocandin resistance is largely due to mutations in the gene encoding β-glucan synthase, but the mode of action is not fully understood. We developed fluorescent probes based on caspofungin, the first clinically approved echinocandin, and studied their cellular biology in *Candida* species, the most common cause of human fungal infections worldwide. Fluorescently labeled caspofungin probes, like the unlabeled drug, were most effective against metabolically active cells. The probes rapidly accumulated in *Candida* vacuoles, as shown by colocalization with vacuolar proteins and vacuole-specific stains. The uptake of fluorescent caspofungin is facilitated by endocytosis: The labeled drug formed vesicles similar to fluorescently labeled endocytic vesicles, the vacuolar accumulation of fluorescent caspofungin was energy-dependent, and inhibitors of endocytosis reduced its uptake. In a panel comprised of isogenic *Candida* strains carrying different β-glucan synthase mutations as well as clinical isolates, resistance correlated with increased fluorescent drug uptake into vacuoles. Fluorescent drug uptake also associated with elevated levels of chitin, a sugar polymer that increases cell-wall rigidity. Monitoring the intracellular uptake of fluorescent caspofungin provides a rapid and simple assay that can enable the prediction of echinocandin resistance, which is useful for research applications as well as for selecting the appropriate drugs for treatments of invasive fungal infections.

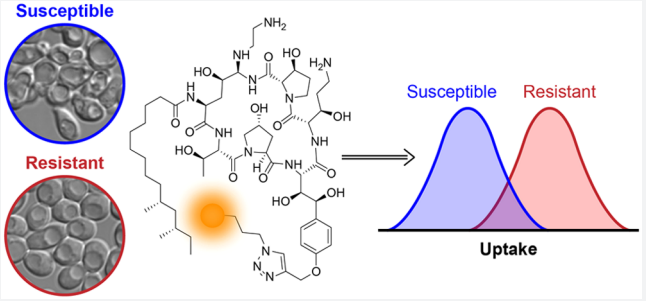

INTRODUCTION

Echinocandins are the most recently approved class of antifungal drugs used for treatment of invasive fungal infections.[1,2] These semisynthetic drugs, developed from fermentation metabolites, are composed of different hexapeptide scaffolds attached to an N-linked lipid chain that have been modified chemically to optimize pharmacokinetic and pharmacodynamic properties.[3−6] The three echinocandins approved for clinical use by the Food and Drug Administration (FDA), namely, caspofungin, micafungin, and anidulafungin (approved in 2001, 2005, and 2006, respectively), are considered among the most effective and best-tolerated antifungals in clinical use against *Candida* species,[7,8] the most frequently encountered fungal pathogens of humans in Western hospitals.[9,10] Rezafungin (CD101), a newly developed echinocandin currently undergoing advanced clinical trials, has an extended half-life enabling a single weekly dose.[11,12]

Echinocandins are currently the only class of clinically approved antifungal drugs that act by inhibiting β-(1 → 3)-glucan synthase (GS), a membrane-bound protein complex essential for fungal cell-wall biosynthesis.[13,14] Importantly, GS is present in fungi but not in animals, which may explain the exceptional safety profile of echinocandins.[3] GS has been implicated as a target for echinocandins by cell-free GS assays showing echinocandin-mediated inhibition of fungal glucan polymer formation from UDP-[^{14}C]-D-glucose.[15,16] Genetic experiments also support this conclusion: Several point-mutation hotspot regions of genes encoding the GS complex subunits are associated with reduced echinocandin susceptibility.[14,17]

Fks1p, an essential component of the GS complex, is an ∼200 kDa protein composed of 16 membrane-spanning domains and encoded by the *FKS1* gene.[18,19] Fks1p is the catalytic subunit that forms the glycosidic linkage in the β-(1 → 3)-D-glucan polymer as was shown by photoaffinity experiments with UDP-D-glucose.[20] Resistance to echinocandins has been associated with point mutation hotspots, and most of these hotspot mutations confer resistance to all three echinocandins in clinical use.[19,21−23] The Fks1 hotspot regions reside in predicted extracellular domains of the protein that are

Received: June 21, 2020
Published: September 9, 2020

https://dx.doi.org/10.1021/acscentsci.0c00813
ACS Cent. Sci. 2020, 6, 1698–1712

thought to bind directly to echinocandins, which act as noncompetitive inhibitors of the GS complex.[4,14]

The sites of mutations that confer resistance to echinocandins, the large size of these drugs (molecular weight (MW) > 1 kDa), and a membrane anchoring lipid segment suggest that echinocandins should localize mainly to the cell surface. Furthermore, the extracellular orientation of the binding site on Fks1p obviates the need for the drug to enter cells to be efficacious.[24,25] However, ^{3}H-labeled-caspofungin accumulates in the cytoplasm of *C. albicans* cells, a process thought to occur via a high-affinity transporter when the concentrations of a drug exceed 1 μg/mL and also through nonselective diffusion across the plasma membrane at higher drug concentrations.[26] A study providing low-resolution images of a Boron-dipyrrmethene (BODIPY)-labeled caspofungin probe suggested that it localized to germ tubes along with possible vesicle involvement in *C. albicans*.[27] This probe was later used in an investigation of the reason for the inherent resistance of the fungal pathogen *Cryptococcus neoformans* to caspofungin.[28] It was demonstrated that the BODIPY-labeled caspofungin probe nonspecifically stained cells of a *C. neoformans* mutant with a damaged plasma membrane while it was barely detectable in the wild-type parent.

Although echinocandins are becoming the drugs of choice for antifungal treatments, they are not always effective.[29−32] This may be due their hydrophobicity and differences in the distribution of these drugs at different infection sites.[33,34] Other possible explanations for efficacy limitations and the continued appearance of echinocandin-tolerant and resistant isolates have not been ruled out. Here, we investigated the mechanisms and dynamics with which echinocandins enter the yeast cells of *Candida* and the relationship between drug uptake and antifungal activity. Fluorescent microscopy techniques are widely applied tools for studying biological processes in living cells and for studying the effects of antifungal drugs against cells of pathogenic fungi.[35−40] Using newly developed fluorescent caspofungin probes, we monitored the subcellular distribution of the drug in live pathogenic yeast cells and the relationship between the degree of intracellular drug internalization and the level of caspofungin resistance in laboratory strains and in clinical isolates.

RESULTS AND DISCUSSION

Design and Synthesis of Fluorescent Caspofungin Probes. The design of fluorescently labeled caspofungin probes developed for this study was based on the specific functionalization of the phenol of 3*S*,4*S*-dihydroxy-L-homotyrosine of the cyclic hexapeptide of caspofungin with a propargyl group to facilitate click reaction-based conjugation of fluorophores. The phenol group was chosen for functionalization, rather than one of the three amines of the cyclic peptide, to avoid a decrease in the overall positive charge of the resultant caspofungin probes under physiological conditions.

The synthesis of propargyl-functionalized caspofungin intermediate **1a** was accomplished in three steps with an overall isolated yield of 45% (Scheme 1A). Briefly, the three amine residues of caspofungin were protected with *tert*-butyloxycarbonyl (BOC) carbamates followed by selective etherification of the phenol with propargyl bromide under basic conditions. Notably, an attempt to remove the BOC carbamates in neat trifluoroacetic acid (TFA) resulted in a mixture of products with the molecular weight of the desired product (1131.38 g/mol), presumably due to isomerization of

Scheme 1. Fluorescent Derivatives of Caspofungin[a]

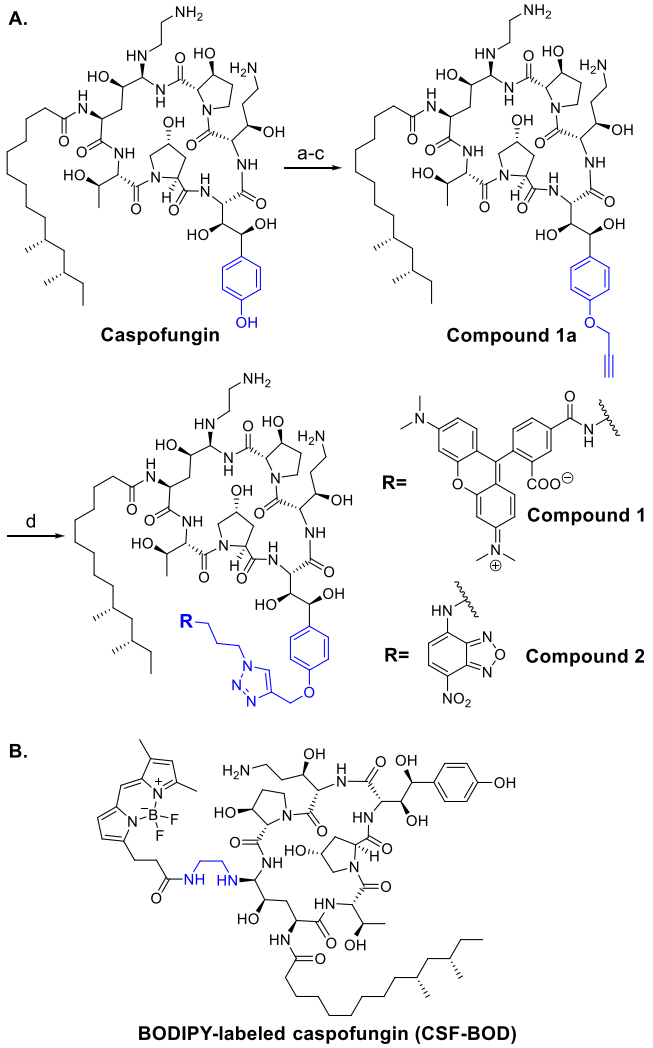

[a](A) Synthesis of fluorescent caspofungin probes **1** and **2**: (a) Boc_2O, dioxane/H_2O, ambient temperature, 48 h, 83%; (b) propargyl bromide in toluene, Cs_2CO_3, DMF, ambient temperature, 14 h, 60%; (c) 37% HCl in H_2O/isopropyl alcohol (1:3, v/v), 2 h, ambient temperature, 90%; (d) azide-functionalized fluorescent dye, $CuSO_4 \cdot 5H_2O$, sodium ascorbate, DMF, ambient temperature; 4 h, 61% for compound **1** and 3 h, 68% for compound **2**. The modified phenol group of 3*S*,4*S*-dihydroxy-L-homotyrosine amino acid is indicated in blue. (B) Structure of BODIPY-labeled caspofungin (**CSF-BOD**).

chiral centers under these acidic conditions. Rapid removal of the BOC groups using hydrogen chloride in aqueous isopropyl alcohol afforded **1a** as a single product in 90% isolated yield (Scheme 1A). The structure of **1a** was confirmed by nuclear Overhauser effect spectroscopy (NOESY) NMR experiments, which showed strong correlations between the aromatic hydrogens of the 3*S*,4*S*-dihydroxy-L-homotyrosine and the protons of the propargyl ether (Figure S3). Finally, azide-functionalized tetramethylrhodamine (TMR) and nitrobenzoxadiazole (NBD) dyes (Scheme S1) were coupled with **1a** under the click reaction conditions to produce fluorescent caspofungin probes **1** (61% isolated yield, absorption 550 nm, and emission 585 nm) and **2** (68% isolated yield, absorption 470 nm, and emission 540 nm), respectively. The four-step synthetic sequences yielded fluorescent caspofungin probes **1** and **2** in ∼27% and ∼30% isolated yields, respectively. The

https://dx.doi.org/10.1021/acscentsci.0c00813
ACS Cent. Sci. 2020, 6, 1698−1712

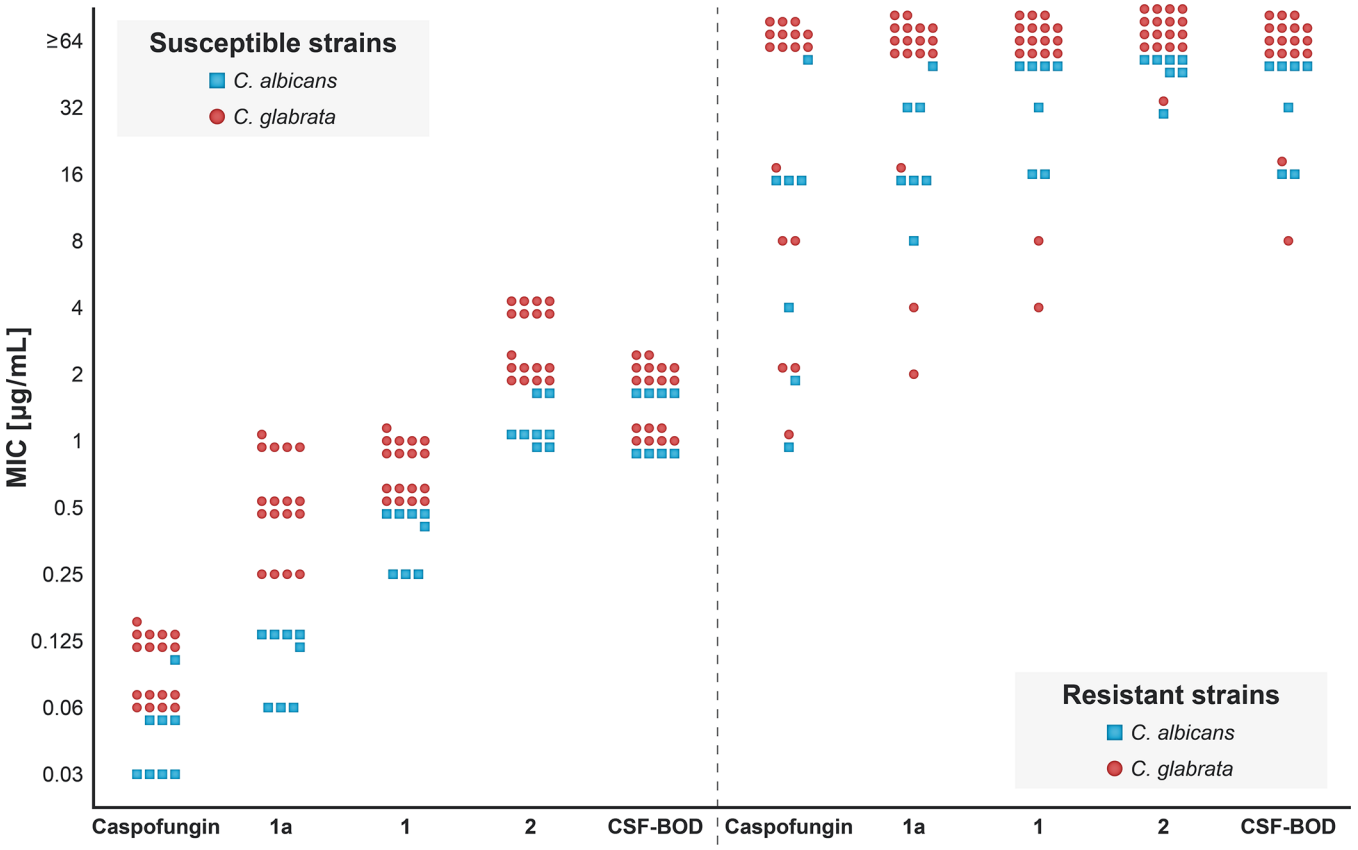

Figure 1. Antifungal activities (MICs) of caspofungin, **CSF-BOD**, and the derivatives **1a**, **1**, and **2**. (blue ■) *C. albicans* strains. (red ●) *C. glabrata* strains. The clinical breakpoints for caspofungin resistance in *C. albicans* and *C. glabrata* are 1 and 0.5 μg/mL, respectively.[8,44]

propargyl-functionalized caspofungin **1a**, which was generated in three steps from the parent drug, is a useful intermediate that can be further modified to generate a large diversity of novel caspofungin derivatives.

BODIPY-labeled caspofungin probe (**CSF-BOD**, Scheme 1B) was synthesized according to the previously reported general procedure.[27] This fluorescent probe was generated by a site-selective attachment of the BODIPY dye (Scheme S2) to the primary amine of the ethylenediamine functionality of the drug via an amide bond. Detailed synthetic and purification procedures as well as characterization and purity analysis of **CSF-BOD** are provided in the Supporting Information. Importantly, of the three fluorescent dyes used for the preparation of the caspofungin probes, NBD fluorescence is pH and environment sensitive,[41] whereas TMR and BODIPY are largely unaffected by pH.[42,43] However, the photostability of the TMR proved to be much higher than that of BODIPY. TMR-labeled caspofungin probe **1** was therefore used as the main probe in this study.

Fluorescent Caspofungin Probes 1 and 2 Retain the Same Spectrum of Antifungal Activity as the Parent Drug. The antifungal activities of the caspofungin derivatives with the modified phenol **1a**, **1**, and **2** were compared to that of caspofungin and **CSF-BOD** using a panel of 49 *C. albicans* and *C. glabrata* strains (Table S1). The panel included American-type culture collection (ATCC) strains and clinical isolates as well a collection of caspofungin-susceptible strains and their corresponding isogenic caspofungin-resistant derivatives. The caspofungin-resistant derivatives were constructed by introducing point mutations within and near the defined hotspots in the *FKS1* and/or *FKS2* genes of the GS complex. The minimal inhibitory concentration (MIC) values for all strains were determined using the broth double-dilution method and are summarized in Figure 1 and Table S2.

The MIC values of **1a** and the TMR-labeled caspofungin probe **1** and those of the NBD-labeled probe **2** were 1−8, 4−16, and 16−64-fold higher than those of the parent caspofungin, respectively (Figure 1, Table S2). The MIC values of **CSF-BOD** were 8−32-fold higher than those of caspofungin against the susceptible strains from the tested panel. Given that the molecular weight and size of the TMR dye is over twofold higher than that of NBD, it was surprising that the MIC values of the NBD-labeled probe **2** were higher than those of the TMR-labeled probe **1**. This difference was more pronounced for *C. albicans* strains than for the *C. glabrata* strains (Figure 1). NBD is a noncharged fluorescent dye, but TMR is zwitterionic. This feature can modulate the binding interactions between the fluorescent probe and its target site in the GS complex and may account for the antifungal efficacy differences between probes **1** and **2**. Importantly, the antifungal activity spectrum of the three fluorescent caspofungin probes was identical to that of caspofungin: Caspofungin-resistant strains were also resistant to **CSF-BOD** and to **1** and **2**, and caspofungin susceptible strains were also susceptible to the probes. This supports that caspofungin and the fluorescent probes share the same mode of action.

Fluorescent Caspofungin Probes Accumulate in the Vacuole of Yeast Cells Via Endocytosis. The subcellular distribution of the fluorescent caspofungin probes was determined for four *C. albicans* and two *C. glabrata* strains

https://dx.doi.org/10.1021/acscentsci.0c00813
ACS Cent. Sci. 2020, 6, 1698−1712

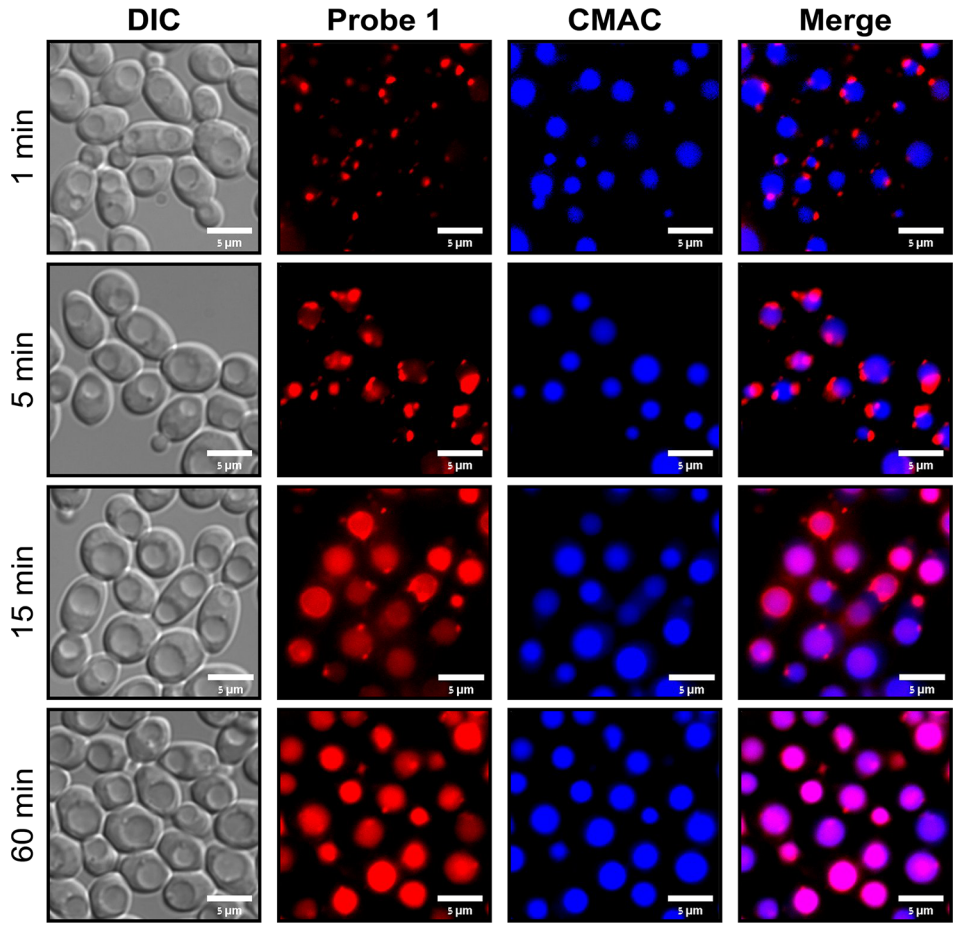

Figure 2. Fluorescent caspofungin probe **1** labels endocytic vesicles and localizes to vacuoles in yeast cells. Representative DIC and fluorescent images of *C. albicans* SC5314 yeast cells incubated with probe **1** for 1, 5, 15, and 60 min. Cells were incubated with probe **1** (1 μM, red) and with the vacuole-specific fluorescent dye CellTracker Blue CMAC (10 μM, blue) in PBS. Scale bars, 5 μm.

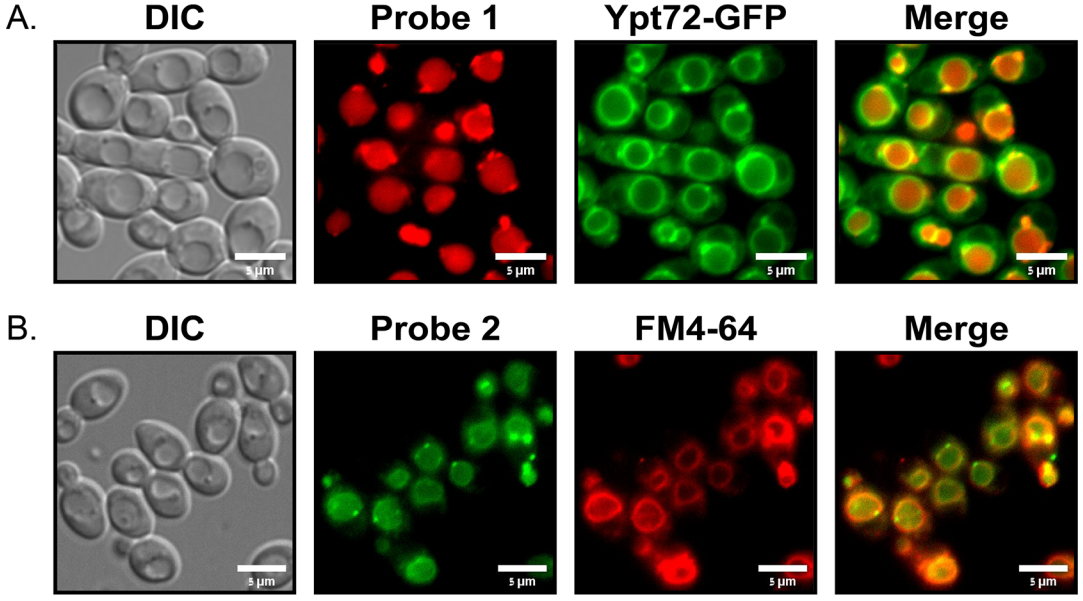

Figure 3. Fluorescent caspofungin probes **1** and **2** localize to vacuoles in yeast cells. (A) DIC and fluorescent images of *C. albicans* CG72 cells expressing Ypt72-GFP (green) incubated with probe **1** (1 μM, red) for 60 min in PBS. (B) DIC and fluorescent images of *C. albicans* SC5314 cells incubated with probe **2** (1 μM, green) and with FM4−64 (1 μg/mL, red) for 60 min in PBS. Scale bars, 5 μm.

using live-cell fluorescence microscopy. Within 15 min, probe **1** localized to vacuoles, as indicated by its colocalization with the vacuole-specific fluorescent dye CellTracker Blue 7-amino-4-chloromethylcoumarin (CMAC)[45,46] (Figures 2 and S16).

https://dx.doi.org/10.1021/acscentsci.0c00813
ACS Cent. Sci. 2020, 6, 1698−1712

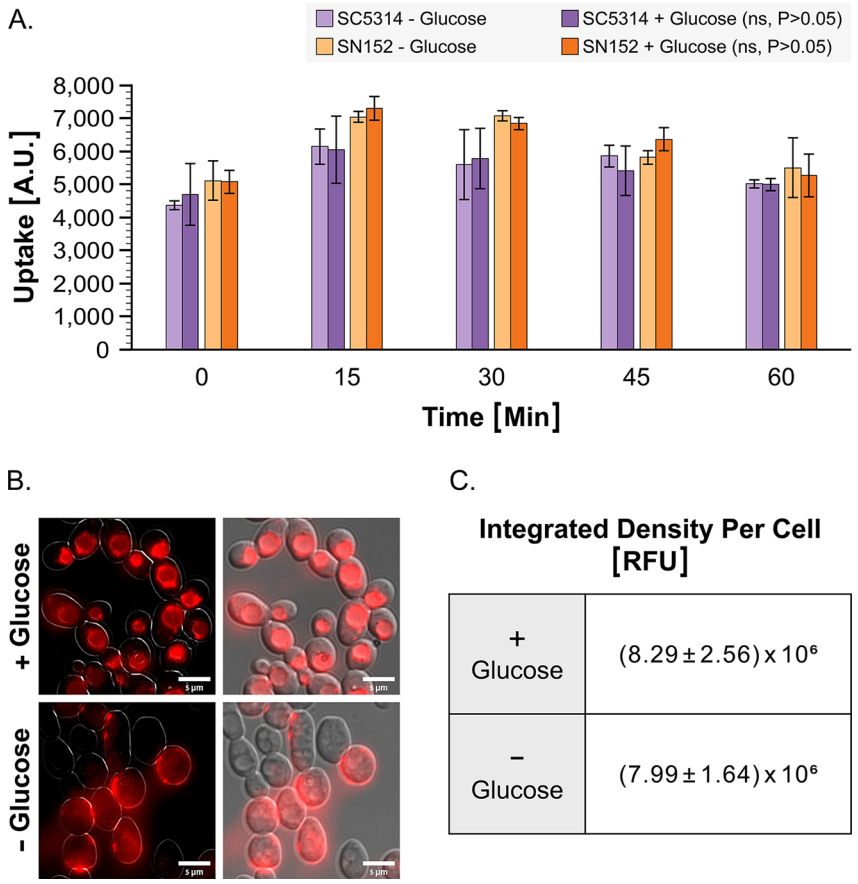

Figure 4. Vacuolar uptake of fluorescent caspofungin probe **1** requires energy. Probe **1** (1 μM in PBS) was added to *C. albicans* SC5314 and SN152 cells maintained with 2% glucose (+ Glucose) or cells starved on PBS without glucose for 4 h (− Glucose). (A) Flow cytometry analysis of the uptake of probe **1** over time (in arbitrary units, A.U.). Data are presented as means ± SD (error bars). Significance was determined by an unpaired *t*-test (ns indicates not significant with $P > 0.05$). (B) Microscopy images of *C. albicans* SC5314 cells treated with probe **1** (red) for 15 min. The DIC images were processed with a Frangi vesselness filter using ImageJ to show the cell borders (left images), merged images of the fluorescent and the DIC channels (right images). Scale bars, 5 μm. (C) Quantification of the fluorescence intensity of probe **1** in cells analyzed by microscopy (as in (B)), with or without 2% glucose. The integrated densities (in relative fluorescent units, RFU) per cell were determined from microscopic images with ImageJ. Data are presented as means ± SD (~3000 cells).

To evaluate how the fluorescent drug transited into vacuoles, we performed a time-lapse analysis that revealed fluorescently labeled vesicular structures, reminiscent of endosomes, within 1 min after the addition of probe **1** (1 μM) (Figure 2, 1 min). These vesicles first accumulated in close proximity to, and then within, the vacuoles (Figure 2, 5 min), ultimately labeling entire vacuoles within 15 min (Figure 2, 15 min). The probe remained concentrated in vacuoles for the remaining duration of the experiments (Figure 2, 60 min). Importantly, the same localization patterns were evident for TMR-based probe **1**, NBD-based probe **2**, and for **CSF-BOD** (Figures S16−S19). No such staining was observed in the yeast cells treated with the azide-functionalized TMR or NBD dyes used for the preparation of probes **1** and **2**, respectively (Figure S20). This supports the idea that the caspofungin scaffold, and not the fluorescent dye segments, drove the subcellular distribution of the fluorescent probes to endocytic vesicles that subsequently fused with vacuoles.

If the caspofungin probes were internalized via endocytosis and accumulated in the vacuole, then in *C.albicans*, the probes should be surrounded by Ypt72, a vacuolar Rab small monomeric GTPase, which localizes primarily to the vacuolar membrane.[47] Additionally, vesicles directed to the vacuole should form a fluorescent pattern of endocytic vesicles similar to that observed in yeast stained with FM4−64, a fluorescent dye that localizes to endocytic vesicles and the vacuolar membrane.[48] Indeed, in *C. albicans* cells that express Ypt72-GFP[47] (strain 7, Table S1), the Ypt72-GFP-labeled vacuolar membrane surrounded probe **1** (Figure 3A and Figure S17), indicating that the probe localizes to the vacuole. A similar pattern was seen with probe **2** relative to FM4−64(Figure 3B), further supporting the idea that the internalization of either of the fluorescent caspofungin probes occurs via endocytosis in *C. albicans*. Incubation with probe **1** for a short period of time (Figure 2, 1−5 min) gave a similar endosomal pattern to that observed in cells stained with FM4−64 (Figure S21, 1−5 min), further supporting the idea that internalization of either of the fluorescent caspofungin probes into *Candida* cells occurs via endocytosis. Endocytosis is an energy-dependent process.[48,49] To ask if the intracellular uptake of fluorescent caspofungin is energy-dependent, we evaluated the effect of glucose on the uptake of probe **1**. Cells from common *C. albicans* yeast laboratory strains (SC5314 and SN152, Table S1) were suspended in phosphate-buffered saline (PBS) with or without 2% glucose. After 4 h of incubation, probe **1** was added to a final concentration of 1 μM, and its cellular uptake was measured by flow cytometry every 15 min for 1 h (Figure 4A). The differences in the uptake of probe **1** in the glucose-rich

https://dx.doi.org/10.1021/acscentsci.0c00813
ACS Cent. Sci. 2020, 6, 1698−1712

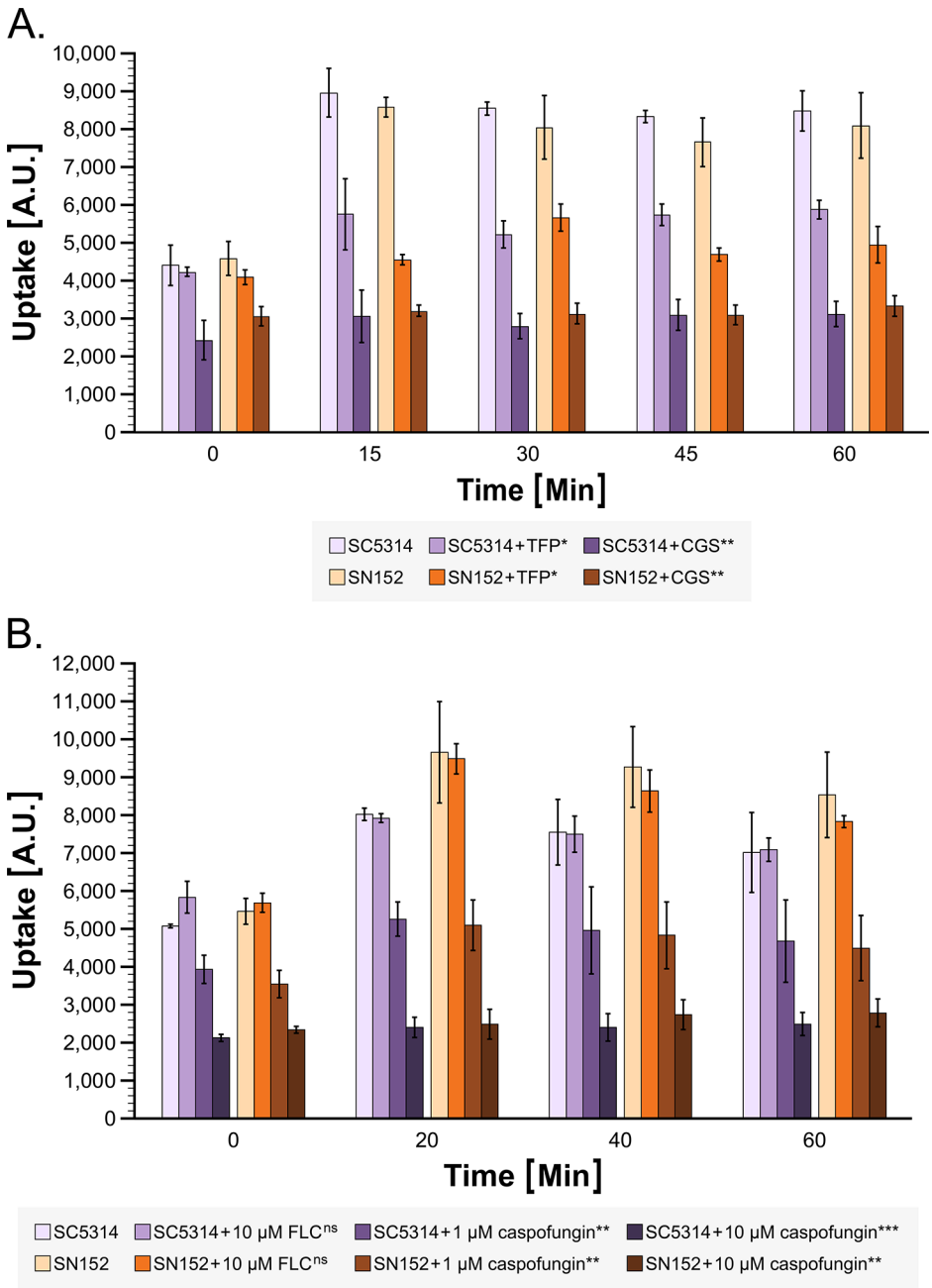

Figure 5. Uptake of fluorescent caspofungin probe **1** is decreased by endocytosis inhibitors and caspofungin addition. (A) Probe **1** (1 μM in PBS) was added to *C. albicans* SC5314 and SN152 cells with or without preincubation with 8 μg/mL of the endocytosis inhibitors TFP or CGS 12066B for 2 h. (B) Probe **1** (1 μM in PBS) was added to *C. albicans* SC5314 and SN152 cells with or without addition of caspofungin (1 μM, 10 μM) or fluconazole (FLC) (10 μM). Data are presented as means ± SD (error bars). Significance was determined by an unpaired *t*-test (* $P \leq 0.05$, ** $P \leq 0.01$, *** $P \leq 0.001$; ns indicates not significant with $P > 0.05$).

PBS solution, relative to the glucose-free PBS, during the 60 min duration of the experiment were not significant (*t*-test: *P*-value > 0.05) (Figure 4A), suggesting that the uptake of **1** might not be energy-dependent.

However, analysis by microscopy provided a different perspective (Figure 4B). In the presence of glucose, probe **1** accumulated in the vacuole (Figure 4B), while in the absence of glucose it accumulated primarily at the cell envelope (Figure 4B). These results support the idea that intracellular uptake of echinocandins is dependent upon endocytosis, which is an energy-dependent process. Furthermore, the fluorescence microscopy results can explain the apparent paradox between the flow cytometry results, which measured fluorescence per cell, irrespective of the probe localization within the cell, and the microscopy results, which noted the differences in intracellular localization: The degree of probe **1** fluorescence at the cell surface in the absence of glucose and within the vacuole in the presence of glucose were of the same magnitude (*t*-test: *P*-value > 0.05) (Figure 4C). These results suggest that echinocandins associate with the cell surface in an energy-independent manner and that their uptake into vacuole-directed vesicles requires energy.

If echinocandin uptake occurs via endocytosis, then inhibitors of endocytosis should inhibit the uptake of

https://dx.doi.org/10.1021/acscentsci.0c00813
ACS Cent. Sci. 2020, 6, 1698−1712

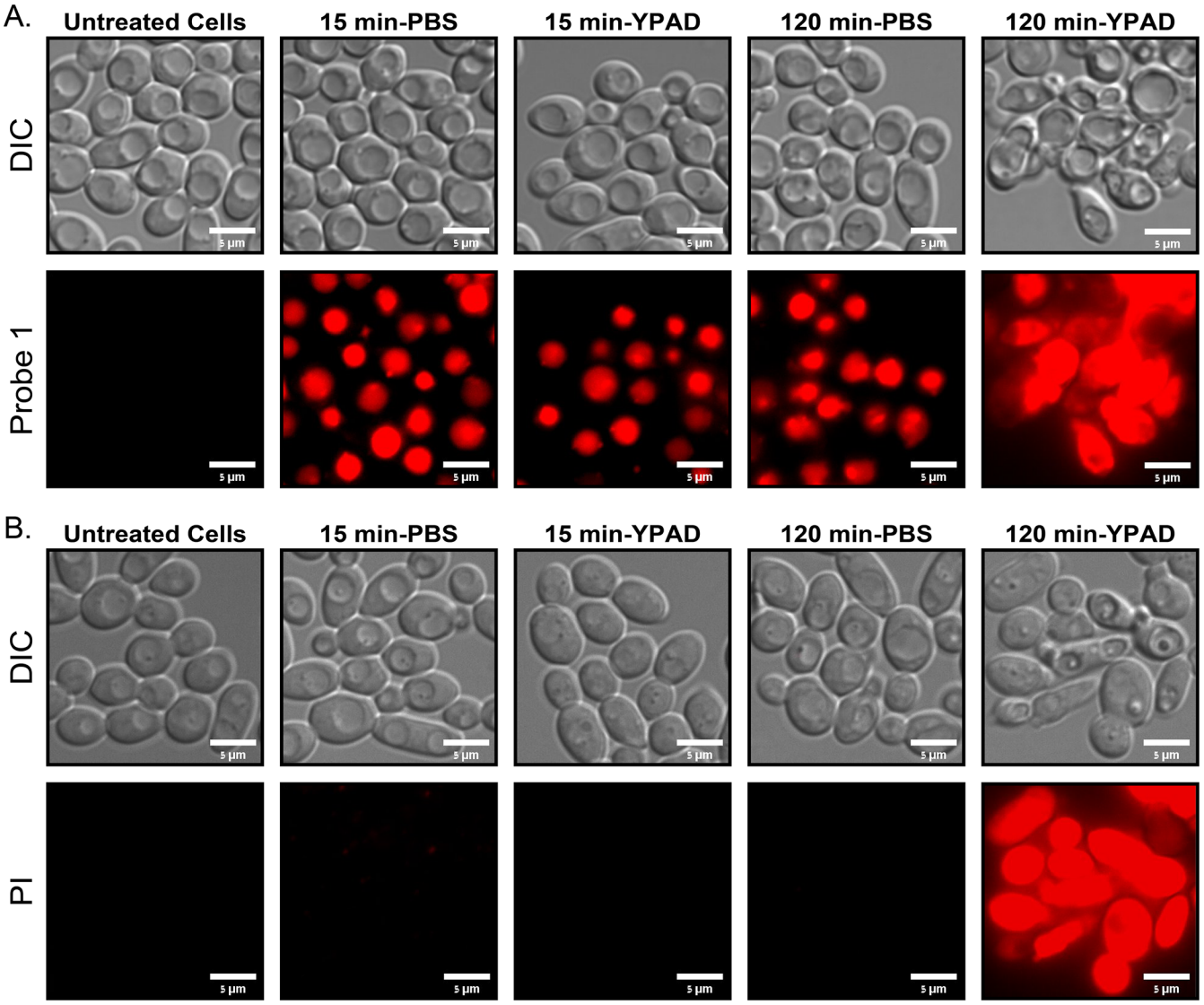

Figure 6. Caspofungin causes plasma membrane permeabilization and the death of dividing cells. (A) DIC and fluorescent images of *C. albicans* SC5314 cells treated with probe **1** (1 μM, red) in PBS or YPAD and untreated cells (no probe **1**). (B) DIC and fluorescent images of cells maintained in PBS or YPAD, treated or not with caspofungin (1 μM) and stained with PI (20 μM, red). Scale bars, 5 μm.

fluorescently labeled caspofungin. The accumulation of probe **1** in *C. albicans* SC5314 and SN152 cells was measured by flow cytometry in the absence and presence of endocytosis inhibitors trifluoperazine (TFP) or pyrroloquinoxaline derivative CGS 12066B (Figure 5A). TFP is a dopamine receptor antagonist,[50] and CGS 12066B is a serotonin-1B receptor agonist,[51] both of which also inhibit endocytosis in *C. albicans*.[52] Both inhibitors modestly reduced growth at the concentration used (8 μg/mL): They primarily slowed the emergence from lag phase (Figure S23).

Notably, both endocytosis inhibitors significantly decreased the uptake of probe **1** relative to the uptake levels in yeast cells not treated with an endocytosis inhibitor, with the effect of CGS 12066B more pronounced than that of TFP (Figure 5A). For example, after 30 min, TFP inhibited the uptake of probe **1** by ~30%, and CGS 12066B inhibited its uptake by ~60% in both *C. albicans* SC5314 and SN152. These results, together with live cell imaging and glucose starvation data, strongly support the idea that the intracellular uptake of fluorescent caspofungin probe **1** occurs within minutes, largely via endocytic vesicles that drive vacuolar accumulation.

To determine if caspofungin competes for cellular uptake with fluorescent probe **1**, both the drug and the probe were added simultaneously to cultures of strains SC5314 and SN152. The uptake of probe **1** was measured by flow cytometry every 15 min for 1 h (Figure 5B). Addition of caspofungin reduced the uptake of probe **1** in a dose-dependent manner. No effect on the uptake of probe **1** was detected in cells co-treated with the antifungal azole drug fluconazole, which inhibits the biosynthesis of the fungal membrane sterol, ergosterol. These results suggest that the endocytic internalization of echinocandins into yeast cells is mediated by the binding of the drug to a membrane protein target, possibly the GS complex. Notably, in the important fungal pathogen *Aspergillus fumigatus*, caspofungin induces dynamic changes in the localization of Fks1p from the membrane to the vacuole.[53] This suggests that endocytic migration of Fks1p from the plasma membrane to the vacuole

https://dx.doi.org/10.1021/acscentsci.0c00813
ACS Cent. Sci. 2020, 6, 1698−1712

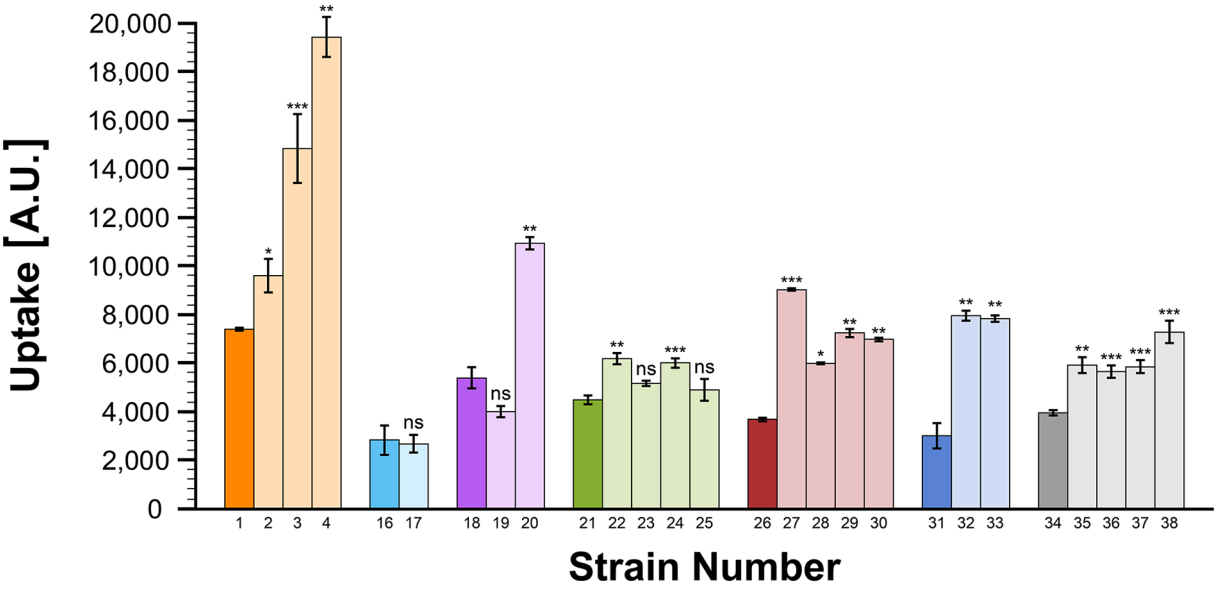

Figure 7. Comparison of caspofungin probe **1** uptake by parental and mutant *C. albicans* (Strains 1−4, Table S1) and *C. glabrata* (Strains 16−38, Table S1) strains carrying *FKS* mutations. Intracellular fluorescence of parental strains (dark colors) and their corresponding mutant strains (light colors) were analyzed by flow cytometry after 15 min of incubation with probe **1** (1 μM). Data are presented as means ± SD (error bars). Significance was determined by an unpaired *t*-test (* $P \leq 0.05$, ** $P \leq 0.01$, *** $P \leq 0.001$; ns indicates not significant with $P > 0.05$).

may be involved, at least in part, in vacuolar accumulation of echinocandins.

Echinocandins Are More Effective against Dividing Yeast Cells than against Quiescent Cells. The localization of probe **1** was very different in *Candida* cells incubated for 2 h in nutrient-rich medium, yeast extract peptone dextrose medium plus adenine (YPAD), than in nutrient-free PBS. In cells maintained in PBS, the probe remained concentrated in vacuoles over the 2 h duration of the experiment (Figure 6A). By contrast, in cells maintained in YPAD, the vacuolar pattern of probe **1** had dispersed after 2 h, and the entire cytoplasm was brightly stained (Figure 6A). Differential interference contrast (DIC) images of cells grown in YPAD and treated with probe **1** revealed larger, more misshapen cells that often appeared to be collapsed, characteristic of dead yeast cells. Thus, the caspofungin probe was relocalized from the vacuole in cells incubated in nutrient-rich growth medium, while cells in PBS retained probe **1** in the vacuole and did not appear to be undergoing cell damage.

To ask if the caspofungin relocalization and apparent cell damage and death is a feature of caspofungin and not only of the fluorescently labeled caspofungin probe **1**, we followed cell viability by staining with propidium iodide (PI), a dye excluded from viable cells. We compared cell viability in the presence and absence of 1 μM unlabeled caspofungin in cells incubated either in PBS or in YPAD. Cells incubated in PBS excluded the PI stain (Figure 6B), indicating that the plasma membrane remained intact and the cells were viable. By contrast, in YPAD medium, cells were viable after 15 min but stained brightly with PI after 2 h. Thus, cells exposed to caspofungin in nutrient-rich conditions become permeable to PI, indicative of cell death. This explains the nonspecific distribution of probe **1** in the cytoplasm after prolonged incubation (Figure 6A). It is also consistent with the idea that plasma membrane permeabilization and cell death are likely accompanied by the loss of structural integrity of organelles, including the vacuoles detected here. YPAD contains nutrients that promote cell growth, whereas PBS only maintains cells in a quiescent state. Cell growth is dependent upon cell-wall expansion, which in turn requires β-glucan production catalyzed by GS. We hypothesize that growing cells are more sensitive to caspofungin, because, when cell-wall integrity is compromised due to loss of GS activity, growth leads to cell deformation, membrane rupture, and cell death. By contrast, when cells are quiescent, the drug remained in vacuoles, and, despite the lack of β-glucan synthesis, the cells remain viable.

Uptake of Fluorescent Probe 1 into Caspofungin-Resistant *Candida* Strains Is Enhanced. We next exploited a number of pairs of isogenic strains in which the parental strains are echinocandin-sensitive and the progeny strains are echinocandin-resistant due to point mutations in the *FKS* genes. This included four *C. albicans* strains (Strains 1−4, Table S1)[54] and a collection of 23 *C. glabrata* strains in six different genetic backgrounds (Strains 16−38, Table S1).[55,56] We first determined the subcellular localization of caspofungin probe **1** in four echinocandin-resistant progeny strains from the panel by microscopy (Figure S22) and found that the probe localized to the vacuole as it did in echinocandin-susceptible strains. We then quantified the dynamics of cellular association with probe **1** by flow cytometry at 15 min intervals for 1 h (Figure 7 and Figure S24). Interestingly, after 15 min, a statistically significant increase in probe **1** uptake was observed in 80% of the resistant strains relative to the corresponding parental strains (Figure 7). Since all of the resistant strains in the panel are mutants in one of the two *FKS* genes that encode GS (Table S1), these results suggest a possible connection between *FKS* mutations and the uptake of probe **1**.

To investigate if increased uptake of probe **1** by echinocandin-resistant strains is a more general phenomenon that spans most genetic backgrounds in addition to those in Figure 7, we scanned a set of *C. albicans* clinical isolates with a broad range of echnocandin susceptibility/resistance (Strains 5−15, Table S1), as well as a set of *C. glabrata* clinical isolates (Strains 39−49, Table S1). Probe **1** uptake for resistant strains was significantly higher than for susceptible strains (*t*-test: *P*-value < 0.05 and <0.0001 for *C. albicans* and *C. glabrata*,

https://dx.doi.org/10.1021/acscentsci.0c00813
ACS Cent. Sci. 2020, 6, 1698−1712

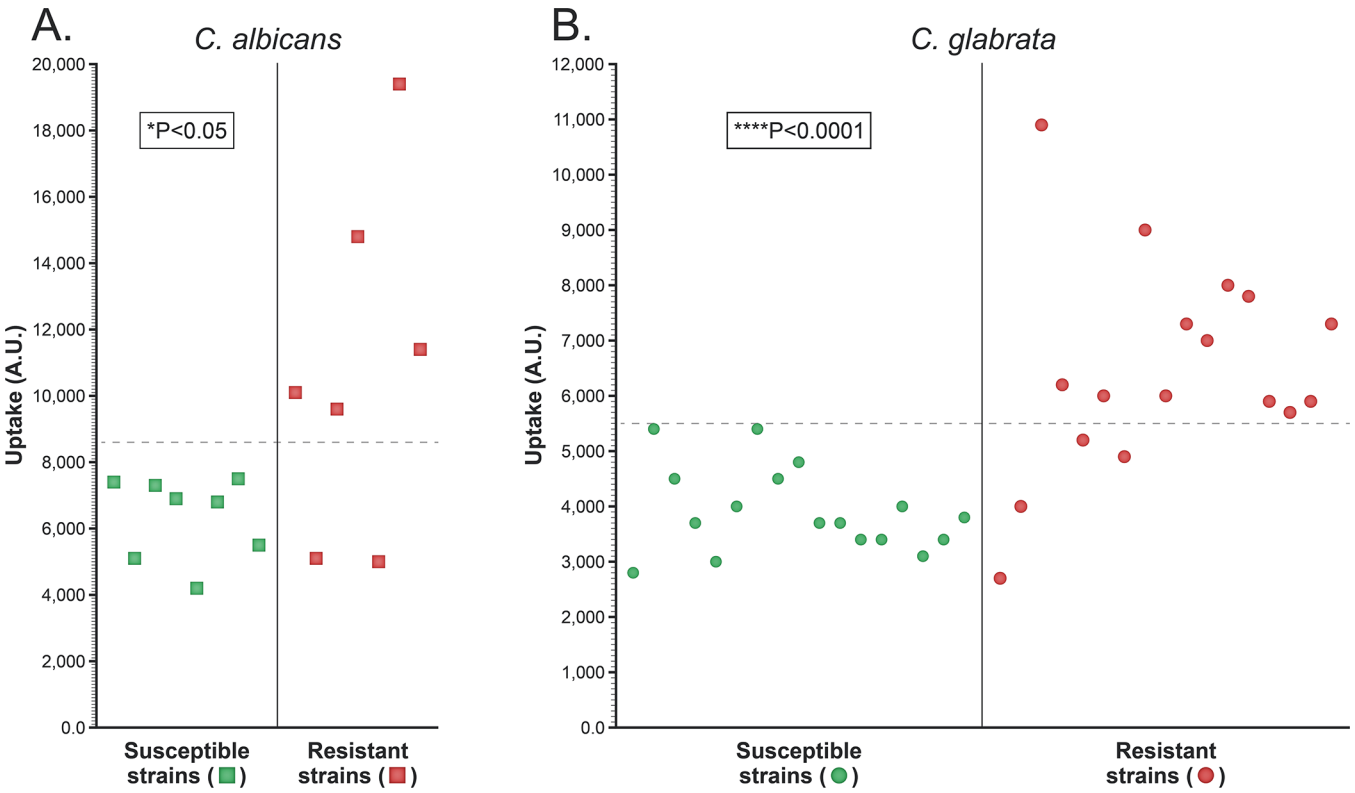

Figure 8. Caspofungin resistance is associated with probe **1** uptake. The uptake of probe **1** was measured after 15 min of incubation with caspofungin-susceptible strains (green, *C. albicans* and *C. glabrata* MIC ≤ 0.25 and 0.12 μg/mL, respectively) and caspofungin-resistant strains (red, *C. albicans* and *C. glabrata* MIC ≥ 1 and 0.5 μg/mL, respectively). Horizontal dashed lines indicate cutoff values defined based upon receiver operating characteristics (ROC). Significance of the difference between the uptake of probe **1** by the group of resistant strains and the group of susceptible strains was determined by an unpaired *t*-test (* $P \leq 0.05$, **** $P \leq 0.0001$).

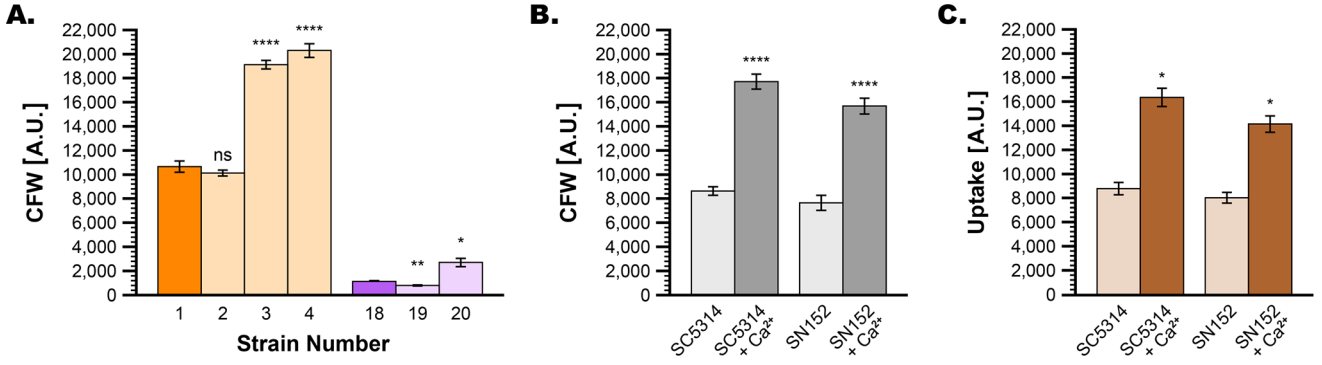

Figure 9. Endocytic vacuolar uptake of fluorescent caspofungin probe **1** is elevated in yeast strains that have high levels of chitin. (A) Comparison of the level of chitin in parental and mutant *C. albicans* (Strains 1−4, Table S1) and *C. glabrata* (Strains 18−20, Table S1). Chitin levels of parental strains (dark colors) and their corresponding mutant strains (light colors) were analyzed by flow cytometry after 30 min of incubation with CFW (25 μg/mL). (B) Comparison of chitin levels (CFW staining) in *C. albicans* SC5314 and *C. albicans* SN152 cells maintained without or with 0.1 M Ca^{2+}. (C) Comparison of probe **1** uptake into *C. albicans* SC5314 and *C. albicans* SN152 cells maintained without or with 0.1 M Ca^{2+}. Data are presented as means ± SD (error bar). Significance was determined by an unpaired *t*-test (* $P \leq 0.05$, ** $P \leq 0.01$, **** $P \leq 0.0001$, and ns indicates not significant with $P > 0.05$).

respectively) (Figure 8). The susceptible *C. albicans* and *C. glabrata* strains had average levels of fluorescence of 6.3 ± 0.5 and 3.9 ± 0.2, respectively, and the resistant strains were 10.8 ± 1.4 and 6.5 ± 0.5, respectively.

Cutoff values defined for probe **1** (1 μM) uptake based upon ROC curves using SPSS software distinguished between caspofungin-sensitive and caspofungin-resistant strains. Importantly, 71% of the *C. albicans* and 77% of the *C. glabrata* echinocandin-resistant strains tested resistant using the calculated cutoff lines (Figure 8). Notably, all of the strains with uptake values above the cutoff lines were confirmed as resistant. Thus, on average, the increased uptake of fluorescent caspofungin probe **1** appears to be associated with echinocandin resistance. The NBD- and BODIPY-labeled caspofungin probes behaved similarly to the TMR-based probe (Figures S25 and S26) in resistant strains relative to the corresponding parental strains. This further supports our hypothesis that the caspofungin scaffold, and not the fluorescent dye or the labeling position on the drug, is responsible for the observed enhanced uptake of the

https://dx.doi.org/10.1021/acscentsci.0c00813
ACS Cent. Sci. 2020, 6, 1698−1712

fluorescent probes in echinocandin-resistant strains. Given that the detection process requires less than 30 min to complete, an assay that monitors fluorescent caspofungin derivative uptake could be used to identify echinocandin-resistant isolates of pathogenic yeast.

Elevated Cell-Wall Chitin Is Associated with Enhanced Fluorescent Caspofungin Probe 1 Uptake into the Vacuoles of Echinocandin-Resistant *Candida*. The fungal cell wall is a dynamic matrix, and a decrease in one of its components is usually compensated by an increase in others.[57,58] It is well-established that caspofungin-mediated inhibition of GS results in increased cell-wall chitin content in *Candida*.[59−61] Elevated cell-wall chitin levels were also detected in *FKS* mutants of *C. albicans* that confer echinocandin resistance.[54,62] Thus, we investigated if elevated levels of probe **1** uptake are associated with elevated levels of cell-wall chitin in echinocandin-resistant *Candida*.

We first measured chitin levels in echinocandin-susceptible *C. albicans* SC5314 and three of its resistant progeny strains (Strains 1−4, Table S1), as well as in echinocandin-susceptible *C. glabrata* CST109 and two of its resistant progeny strains (Strains 18−20, Table S1). Chitin levels were measured by flow cytometry as the fluorescent signal in cell samples that were stained with the chitin-specific dye calcofluor white (CFW).[63] Elevated chitin levels were observed in the cells of the echinocandin-resistant *C. albicans* progeny strains relative to their susceptible parents, with the exception of strain 2 (Figure 9A). Similarly, a significant increase in chitin was detected in the *C. glabrata* progeny strain 20 but not of progeny strain 19 (Figure 9A). Importantly, the chitin levels in the strains could be associated with their uptake of fluorescent caspofungin probe **1**. Indeed, the two strains (2 and 19) that did not show elevated chitin staining (Figure 9A) also showed very little difference in their uptake of probe **1** relative to their parent strains (Figure 7).

Calcium enhances the chitin content in *C. albicans* cell walls and reduces caspofungin susceptibility.[64,65] To further establish the relationship between caspofungin susceptibility, chitin production, and the uptake of fluorescent caspofungin probe **1**, caspofungin-susceptible *C. albicans* cells (SC5314 and SN152) were preincubated in YPAD containing 0.1 M Ca^{2+} for 18 h, to stimulate the elevation of chitin content in the cell wall, and then were stained with CFW or with probe **1** and analyzed by flow cytometry. We detected an approximately twofold elevation in chitin levels (Figure 9B), along with an approximately twofold elevation in the uptake of probe **1** (Figure 9C), when the medium was supplemented with Ca^{2+} relative to yeast cells maintained in the absence of added Ca^{2+}. Of note, in *C. albicans* similar fluorescent signal intensities were measured in cells stained with CFW or with probe **1**. In *C. glabrata*, however, the signal intensity of CFW was significantly lower than that of probe **1**. Thus, in *C. glabrata*, CFW appears to be a less-sensitive indicator of caspofungin resistance than probe **1** uptake (compare strains 18−20 in Figure 9 and Figure 7). The percentage of chitin in the cell wall of *C. glabrata* is significantly lower than that in *C. albicans*.[66] This likely explains the observation that, in *C. glabrata*, the chitin stain CFW is a less-sensitive indicator of caspofungin resistance.

These results suggest that increasing chitin levels in the cell wall results in the increased uptake of echinocandins into vacuoles via endocytosis. Chitin enhances cell-wall rigidity and the ability of the cell wall to counter intracellular turgor pressure, which can affect the equilibrium between endocytic and exocytic processes.[67] This may offer a plausible explanation for the observed elevation in the endocytic vacuolar uptake of fluorescent caspofungin probe **1** in echinocandin-resistant yeast that have higher levels of cell-wall chitin.

CONCLUSION

Through a facile four-step synthesis, we developed fluorescently labeled probes of caspofungin, a member of the echinocandin class of antifungal drugs, and validated their antifungal activity. These probes enable live-cell imaging by microscopy and flow cytometry and were used to characterize the organellar sites of drug localization and drug uptake into *Candida* isolates. We found that the fluorescent drug accumulates in vacuoles within minutes. Cellular uptake occurs via endocytosis, as uptake of the fluorescent drug was energy-dependent and reduced by endocytosis inhibitors. The uptake of fluorescently labeled caspofungin was reduced in the presence of the parent drug, suggesting that endocytic internalization of echinocandins is mediated via a membrane protein, possibly the GS complex. Notably, time-dependent subcellular distribution of the fluorescent drug indicated that echinocandins cause more cell death under conditions that promote rapid yeast cell growth; when cells were maintained in glucose-free buffer, the drug accumulated and remained in vacuoles. This important observation illustrates that echinocandins are effective against metabolically active and dividing yeast and that their maintenance within the vacuole does not kill slowly dividing and/or dormant cells. It remains unclear whether the presence of drug in the vacuole contributes to cell death. It is possible that vacuolar trafficking of echinocandins is simply a byproduct of membrane turnover via endocytosis, which may be accelerated in cells with elevated levels of cell-wall chitin. Given that a minority of the echinocandin-resistant isolates do not have abnormally high chitin levels or increased probe **1** uptake, we think that vacuolar localization is likely due to membrane turnover.

We discovered that the level of fluorescent caspofungin uptake into yeast cells was significantly higher in most echinocandin-resistant strains compared to parental echinocandin-susceptible *Candida* strains. This phenomenon is associated with the level of chitin in the *Candida* cell wall. The uptake of the fluorescent drug was significantly higher in 75% of the echinocandin-resistant strain relative to the susceptible strains among the tested panel of 49 *Candida* strains. Furthermore, we found that calcium-mediated stimulation of chitin production also increased fluorescent probe **1** uptake.

Echinocandin resistance has emerged over the recent years in most clinically relevant *Candida* species, and it is particularly common in *C. glabrata* clinical isolates. Of clinical relevance, the quantification of probe **1** uptake can identify isolates that are echinocandin-resistant and provide an assay that is rapid and more sensitive than assays based on CFW staining of chitin in *C. glabrata*. This further enhances the usefulness of fluorescent caspofungin probes for identifying echinocandin resistance in these important pathogenic yeasts.

To conclude, the fluorescently labeled caspofungin probes reported herein offer a new and useful research tool for the study of the biological activity of members of the echinocandin class of antifungal drugs. These drugs are critical for treating invasive, life-threatening fungal infections. Enhanced vacuolar uptake of the fluorescent caspofungin probes by echinocandin-

https://dx.doi.org/10.1021/acscentsci.0c00813
ACS Cent. Sci. 2020, 6, 1698−1712

resistant pathogenic yeast can be harnessed to facilitate rapid prediction of drug resistance and assist in devising optimal drug treatments for invasive fungal infections.

MATERIALS AND METHODS

General Chemistry Methods and Instrumentation. ^{1}H NMR spectra (including one-dimensional total correlation spectroscopy (1D-TOCSY) and two-dimensional (2D) NOESY) were recorded on BrukerAvance 400 or 500 MHz spectrometers. ^{13}C NMR spectra were recorded on Bruker-Avance 400 or 500 MHz spectrometers at 100 or 125 MHz. Chemical shifts (reported in ppm) were calibrated to CD_3OD (^{1}H: δ = 3.31, ^{13}C: δ = 49.0). Multiplicities are reported using the following abbreviations: b = broad, s = singlet, d = doublet, t = triplet, dd = doublet of doublets, ddd = doublet of doublet of doublets, td = triplet of doublets, m = multiplet. Coupling constants (J) are given in hertz. High-resolution electrospray ionization (HRESI) mass spectra were measured on a Waters Synapt instrument. Low-resolution electrospray ionization mass spectra (ESI-MS) were measured on a Waters 3100 mass detector. Chemical reactions were monitored by thin-layer chromatography (TLC) (Merck, Silica gel 60 F254). Visualization was achieved using a cerium molybdate stain (5 g of $(NH_4)_2Ce(NO_3)_6$, 120 g of $(NH_4)_6Mo_7O_{24}{\cdot}4H_2O$, 80 mL of H_2SO_4, 720 mL of H_2O) or with a UV lamp. All chemicals, unless otherwise stated, were obtained from commercial sources. Compounds were purified using Geduran Si 60 chromatography (Merck). The preparative reverse-phase high-pressure liquid chromatography (RP-HPLC) system used was an ECOM system equipped with a 5 μm, C-18 Phenomenex Luna Axia column (250 mm × 21.2 mm). Analytical RP-HPLC was performed on a VWR Hitachi instrument equipped with a diode array detector and an Alltech Apollo C18 reversed-phase column (5 m, 4.6 × 250 mm). The flow rate was 1 mL/min. Solvent A was 0.1% TFA in water, solvent B was acetonitrile. The SpectraMax i3x Platform spectrophotometer from Molecular Devices was used for fluorescence measurements.

Compound 1. Compound **1a** (25 mg, 0.02 mmol) was dissolved in dimethylformamide (DMF) (2 mL) and treated with azide-functionalized TMR[68] (20.5 mg, 0.04 mmol, 2 equiv). A catalytic amount of $CuSO_4{\cdot}5H_2O$ and sodium ascorbate were added to the solution. The solution was stirred at ambient temperature for 4 h. Reaction progress was monitored by ESI-MS following the disappearance of the starting material (**1a**: $[M-H]^-$, m/z 1129.46) and the formation of **1** ($[M-H]^-$, m/z 1642.59). Upon completion, the solvent was removed under vacuum. The residue was purified by preparative RP-HPLC (mobile phase: acetonitrile in H_2O (containing 0.1% trifluoroacetic acid), gradient from 10% to 90%; flow rate: 15 mL/min) to afford the hydrochloride salt of compound **1** (21 mg, 61%) as a red powder. HRESI-MS m/z calculated for $C_{83}H_{119}N_{16}O_{19}$, 1643.8837; found $[M]^+$, 1643.8831. ^{1}H NMR (400 MHz, CD_3OD) δ 8.78 (d, J = 1.9 Hz, 1H, TMR), 8.26 (dd, J = 8.0, 1.8 Hz, 1H, TMR), 8.16 (s, 1H, H-4), 7.54 (d, J = 7.9 Hz, 1H, TMR), 7.24 (d, J = 8.6 Hz, 2H, H-1), 7.16 (dd, J = 9.5, 1.1 Hz, 2H, TMR), 7.07 (ddd, J = 9.6, 2.4, 0.8 Hz, 2H, TMR), 6.98−7.03 (m, 4H, H-2, TMR), 5.18 (s, 2H, H-3), 5.02 (d, J = 3.2 Hz, 1H), 4.95 (m, 2H), 4.54−4.69 (m, 5H), 4.51 (dd, J = 12.9, 4.5 Hz, 1H), 4.32−4.40 (m, 2H), 4.31 (d, J = 1.6 Hz, 1H), 4.21−4.28 (m, 2H), 4.14−4.21 (m, 1H), 4.04−4.11 (m, 1H), 4.01 (dd, J = 11.0, 2.9 Hz, 1H), 3.77−3.91 (m, 3H), 3.55 (td, J = 6.5, 1.4 Hz, 2H), 3.00−3.22 (m, 6H), 2.40−2.49 (m, 1H), 2.24−2.37 (m, 5H), 1.96−2.17 (m, 5H), 1.80−1.92 (m, 1H), 1.57−1.67 (m, 2H), 1.24−1.53 (m, 15H), 1.19 (d, J = 6.1 Hz, 3H), 1.03−1.15 (m, 2H), 0.83−0.98 (m, 10H). ^{13}C NMR (125 MHz, CD_3OD) δ 176.7, 174.3, 173.8, 173.4, 172.8, 172.7, 168.9, 168.3, 167.5, 160.7, 159.6, 159.0, 158.9, 145.0, 138.1, 137.4, 135.0, 133.0, 132.3, 131.9, 131.3, 129.6, 125.6, 115.9, 115.6, 114.7, 97.5, 77.4, 75.4, 75.0, 72.3, 71.3, 68.9, 68.6, 68.3, 65.0, 62.8, 62.5, 58.3, 57.1, 56.1, 56.0, 50.7, 47.1, 45.9, 43.1, 40.9, 39.0, 38.5, 38.4, 38.1, 36.9, 35.6, 34.6, 32.9, 31.2, 31.1, 30.9, 30.8, 30.5, 30.3, 28.0, 27.1, 20.7, 20.2, 19.9, 11.5.

Compound 2. Compound **1a** (25 mg, 0.02 mmol), dissolved in DMF (2 mL) and treated with azide-functionalized NBD[69] (10.5 mg, 0.04 mmol, 2 equiv). Catalytic amounts of $CuSO_4{\cdot}5H_2O$ and sodium ascorbate were added to the solution. The solution was stirred at ambient temperature for 3 h. The reaction progress was monitored by ESI-MS following the disappearance of the starting material (**1a**: $[M-H]^-$, m/z 1129.46) and the formation of **2** ($[M-H]^-$, m/z 1392.52). Upon completion, the solvent was removed under vacuum. The residue was purified by preparative RP-HPLC (mobile phase: acetonitrile in H_2O (containing 0.1% TFA), gradient from 10% to 90%; flow rate: 15 mL/min) to afford the hydrochloride salt of compound **2** (20 mg, 68%) as a yellow powder. HRESI-MS m/z calculated for $C_{64}H_{100}N_{17}O_{18}$, 1394.7432; found $[M + H]^+$ 1394.7423. ^{1}H NMR (400 MHz, CD_3OD) δ 8.51 (d, J = 8.7 Hz, 1H, NBD), 8.09 (s, 1H, H-4), 7.24 (d, J = 8.7 Hz, 2H, H-1), 6.99 (d, J = 8.7 Hz, 2H, H-2), 6.26 (d, J = 8.8 Hz, 1H, NBD), 5.17 (s, 2H, H-3), 5.09 (bs, 1H), 5.02 (d, J = 3.2 Hz, 1H), 4.93 (s, J = 6.2 Hz, 1H), 4.54−4.69 (m, 5H), 4.51 (dd, J = 12.8, 4.6 Hz, 1H), 4.32−4.39 (m, 2H), 4.30 (d, J = 1.7 Hz, 1H), 4.27 (d, J = 5.1 Hz, 1H), 4.20−4.26 (m, 2H), 4.04−4.11 (m, 1H), 4.01 (dd, J = 11.0, 2.9 Hz, 1H), 3.78−3.90 (m, 3H), 3.60 (bs, 2H), 3.28−3.02 (m, 6H), 2.36−2.50 (m, 3H), 2.23−2.35 (m, 3H), 1.97−2.20 (m, 5H), 1.81−191 (m, 1H), 1.55−1.67 (m, 2H), 1.23−1.50 (m, 15H), 1.19 (d, J = 6.1 Hz, 3H), 1.05−1.16 (m, 2H), 0.84−0.98 (m, 10H). ^{13}C NMR (125 MHz, CD_3OD) δ 176.7, 174.4, 173.7, 173.4, 172.8, 172.7, 168.9, 159.6, 145.9, 145.5, 145.2, 138.4, 135.0, 129.6, 125.6, 116.0, 99.9, 77.4, 75.4, 75.0, 72.4, 71.3, 68.8, 68.3, 65.2, 62.8, 62.4, 58.3, 57.1, 56.1, 56.0, 50.7, 47.1, 45.9, 43.1, 39.1, 38.5, 38.2, 38.1, 36.9, 35.7, 34.6, 32.9, 31.2, 31.1, 30.8, 30.6, 30.3, 29.7, 28.0, 27.1, 20.7, 20.2, 19.9, 11.6.

Preparation of Stock Solutions of the Tested Compounds. The antifungal drug caspofungin, purchased from S.L. Moran Ltd., and compounds **1a**, **1**, **2**, and **CSF-BOD** were dissolved in anhydrous ethanol to 5 mg/mL or 1 mM. CellTracker Blue CMAC, FM4−64, and PI were purchased from Thermo Fisher and dissolved in dimethyl sulfoxide (DMSO) (10 mM), ddH_2O (5 μg/mL), and ddH_2O (20 mg/mL), respectively. CFW (1 mg/mL) was purchased from Sigma-Aldrich. TFP and CGS 12066B were purchased from Sigma-Aldrich and dissolved in DMSO (5 mg/mL).

***Candida* Strains.** The laboratory and clinical isolates and ATCC strains used in this study are listed in Table S1. Three *FKS* mutants derived from *C. albicans* SC5314[54] and a collection of 17 *FKS* mutants derived from six different genetic backgrounds of *C. glabrata* strains[55,56] were used in this study. Resistant progenies of *C. glabrata* strains were obtained by in vitro evolution. Susceptible strains belonging to different *C. glabrata* clades were serially transferred in liquid medium (YPD) every 3 d for 18 passages and were exposed to increasing concentrations of anidulafungin every two passages

https://dx.doi.org/10.1021/acscentsci.0c00813
ACS Cent. Sci. 2020, 6, 1698−1712

(increments: 0, 0.016, 0.032, 0.064, 0.128, 0.256, 0.512, 1.024, 2.048, and 4.096 μg/mL). Single-colony isolates selected at the last drug concentration were used in this project.

Minimal Inhibitory Concentration Broth Double-Dilution Assay. *Candida* strains were streaked from glycerol stock onto YPAD agar plates and grown for 24 h at 30 °C. Colonies were suspended in 1 mL of PBS and diluted to 2 × 10^{-4} optical density (OD_{600}) in flat-bottom 96-well microplates (Corning) with YPAD broth containing a gradient of twofold dilutions per tested compound with concentrations ranging from 64 to 0.03 μg/mL (5 mg/mL stock solution). Control wells with no drug and blank wells without yeast cells containing YPAD were prepared. MIC values (Table S2) were determined after 48 h at 30 °C by measuring the OD_{600} using a plate reader (Infinite M200 PRO, Tecan). MIC values were defined as the point at which the OD_{600} was reduced by at least 80% compared to the no-drug control wells. Each concentration was tested in triplicate, and the results were confirmed by two independent sets of experiments.

Effect of Endocytosis Inhibitors on *Candida* Growth. To evaluate the effect of TFP and CGS 12066B on the *Candida* growth, 96-well microplates were prepared using the same protocol as described for MIC determination. Plates were incubated for 24 h at 30 °C with shaking in a plate reader (Infinite M200 PRO, Tecan), and the optical density (OD_{600}) was recorded every 40 min.

Live Cell Imaging. *Candida* strains were streaked from glycerol stocks onto YPAD agar plates and grown for 24 h at 30 °C. Colonies were grown in 3 mL of YPAD broth for 24 h at 30 °C with shaking in tubes. Cultures were diluted 1:100 and incubated in YPAD broth for 2 h at 30 °C with shaking until log-phase growth was observed. Cultures were then centrifuged, washed with PBS buffer, and resuspended in PBS buffer. For experiments in YPAD, the cells were stained directly from the log phase. The cells were incubated with probe **1** or **2** or **CSF-BOD** at a final concentration of 1 μM and stained with CellTracker Blue CMAC (10 μM) or FM4−64 (1 μg/mL) at 30 °C with shaking in dark over a 2 h time course. For experiments with PI, the cells were incubated with caspofungin (1 μM) and stained with PI (20 μM). A 2 μL aliquot of a *Candida* cell sample washed with PBS was placed on a glass slide and covered with a glass coverslip. Cells were imaged on a Nikon Ti microscope equipped with a Plan Apo VC 100× Oil objective and a Zyla 5.5 sCMOS camera (Andor) using NIS elements Ar software. The bandpass filter sets used to image probe **1**, TMR-azide, FM4−64, and PI had an excitation wavelength of 560/20 nm and an emission wavelength of 629.5/37.5 nm. To image probe **2**, NBD-azide, **CSF-BOD**, BODIPY methyl ester, and Ypt72-GFP, the excitation wavelength was 470/20 nm, and the emission wavelength was 525/25 nm. For CellTracker Blue CMAC, an excitation wavelength of 350/25 nm and an emission wavelength of 460/25 nm were used. Images were processed using ImageJ.

Flow Cytometry Analysis. *Candida* strains were streaked from glycerol stock onto YPAD agar plates and grown for 24 h at 30 °C. Colonies were grown in 3 mL of YPAD broth for 24 h at 30 °C with shaking. Cultures were diluted 1:100 and incubated in YPAD broth for 2 h at 30 °C with shaking. For experiments with endocytosis inhibitors, the cells were incubated during this 2 h period in the absence or the presence of 8 μg/mL endocytosis inhibitors TFP or CGS 12066B. After the incubation, the cultures were centrifuged, washed with PBS buffer, and resuspended in PBS buffer. For the starvation experiments, the cells were suspended in PBS buffer with or without 2% glucose and incubated for 4 h. Probe **1** was added to a final concentration of 1 μM, and samples were incubated at 30 °C with shaking in dark. Next, 20 μL from each the culture was added to 180 μL of 50 mM Tris-HCl, pH 8.0, 50 mM ethylenediaminetetraacetic acid (EDTA) in round-bottom 96-well microplates. Samples were analyzed every 15 min for 1 h by flow cytometry. For CFW staining, we added CFW to a final concentration of 25 μg/mL. Flow cytometry data were collected from 25 000 to 35 000 cells per time point using Y1 laser excitation (excitation at 561 nm and emission at 585/15 nm) for probe **1**, B1 laser excitation (excitation at 488 nm and emission at 525/25 nm) for probe **2** and **CSF-BOD**, and V1 laser excitation (excitation at 405 nm and emission at 450/50 nm) for CFW on an MACSQuant flow cytometer. Analysis was performed using FlowJo 8.7 software. Results were confirmed by three independent sets of experiments.

Calcium-Based Induction of Cell-Wall Chitin Content. We used Ca^{2+} to increase the chitin content in *C. albicans* as described previously.[64,65] *C. albicans* strains SC5314 and SN152 were streaked from glycerol stock onto YPAD agar plates and grown for 24 h at 30 °C. Colonies were grown in YPAD broth with and without 0.1 M $CaCl_2$ for 18 h at 30 °C with shaking in tubes. Cultures were diluted 1:100 and incubated in YPAD broth with and without 0.1 M $CaCl_2$ for 4 h at 30 °C with shaking. Samples were then centrifuged, washed with PBS buffer, and resuspended in PBS buffer. Test compound (probe **1** or CFW) was added to the desired final concentration, and the experiments were continued as described in the flow cytometry section.

Statistical Analyses. Data are presented as means (two or more replicates) ± standard deviation (SD) (error bars). The significance was determined by an unpaired two-tailed *t*-test using Microsoft Excel 2016. The significance was assigned with $P > 0.05$ not significant. Specificities and sensitivities were calculated based on ROC curves using SPSS software.

■ ASSOCIATED CONTENT

Supporting Information

The Supporting Information is available free of charge at https://pubs.acs.org/doi/10.1021/acscentsci.0c00813.

Detailed synthetic schemes and procedures; ^1H and ^{13}C NMR assignments and high-resolution MS data for intermediate compounds; ^1H and ^{13}C NMR and 2D NOESY spectra; analytic HPLC chromatograms; absorption and emission spectra; yeast strains information; MIC values; live cell imaging data; growth curves; and flow cytometry analysis data (PDF)

■ AUTHOR INFORMATION

Corresponding Authors

Judith Berman − *School of Molecular Cell Biology and Biotechnology, George Wise Faculty of Life Sciences, Tel Aviv University, Tel Aviv 6997801, Israel;* orcid.org/0000-0002-8577-0084; Email: jberman@tauex.tau.ac.il

Micha Fridman − *School of Chemistry, Raymond & Beverly Sackler Faculty of Exact Sciences, Tel Aviv University, Tel Aviv 6997801, Israel;* orcid.org/0000-0002-2009-7490; Email: mfridman@tauex.tau.ac.il

https://dx.doi.org/10.1021/acscentsci.0c00813
ACS Cent. Sci. 2020, 6, 1698−1712

Authors

Qais Z. Jaber − *School of Chemistry, Raymond & Beverly Sackler Faculty of Exact Sciences, Tel Aviv University, Tel Aviv 6997801, Israel;* orcid.org/0000-0001-6780-9494

Maayan Bibi − *School of Molecular Cell Biology and Biotechnology, George Wise Faculty of Life Sciences, Tel Aviv University, Tel Aviv 6997801, Israel*

Ewa Ksiezopolska − *Barcelona Supercomputing Centre (BSC−CNS), Barcelona 08034, Spain; Institute for Research in Biomedicine, The Barcelona Institute of Science and Technology, Barcelona 08028, Spain*

Toni Gabaldon − *Barcelona Supercomputing Centre (BSC−CNS), Barcelona 08034, Spain; Institute for Research in Biomedicine, The Barcelona Institute of Science and Technology, Barcelona 08028, Spain; Catalan Institution for Research and Advanced Studies, Barcelona 08010, Spain;* orcid.org/0000-0003-0019-1735

Complete contact information is available at: https://pubs.acs.org/10.1021/acscentsci.0c00813

Notes

The authors declare no competing financial interest.

■ ACKNOWLEDGMENTS

We thank D. Perlin, D. Sanglard, R. Ben-Ami, C. Fairhead, B. Vincent, J. Usher, D. Soll, and S. Lindquist for providing the *Candida* strains. This work was supported by the Israel Science Foundation, Grant Nos. 179/19 (to M.F.) and 997/18 (to J.B.).

■ REFERENCES

(1) Perfect, J. R. The Antifungal Pipeline: A Reality Check. *Nat. Rev. Drug Discovery* **2017**, *16*, 603−616.

(2) Letscher-Bru, V.; Herbrecht, R. Caspofungin: The First Representative of a New Antifungal Class. *J. Antimicrob. Chemother.* **2003**, *51*, 513−521.

(3) Patil, A.; Majumdar, S. Echinocandins in Antifungal Pharmacotherapy. *J. Pharm. Pharmacol.* **2017**, *69*, 1635−1660.

(4) Lee, Y.; Puumala, E.; Robbins, N.; Cowen, L. E. Antifungal Drug Resistance: Molecular Mechanisms in *Candida albicans* and Beyond. *Chem. Rev.* **2020**. DOI: 10.1021/acs.chemrev.0c00199.

(5) Jiang, W.; Cacho, R. A.; Chiou, G.; Garg, N. K.; Tang, Y.; Walsh, C. T. EcdGHK Are Three Tailoring Iron Oxygenases for Amino Acid Building Blocks of the Echinocandin Scaffold. *J. Am. Chem. Soc.* **2013**, *135* (11), 4457−4466.

(6) Cacho, R. A.; Jiang, W.; Chooi, Y. H.; Walsh, C. T.; Tang, Y. Identification and Characterization of the Echinocandin b Biosynthetic Gene Cluster from Emericella Rugulosa NRRL 11440. *J. Am. Chem. Soc.* **2012**, *134* (40), 16781−16790.

(7) Eschenauer, G.; Depestel, D. D.; Carver, P. L. Comparison of Echinocandin Antifungals. *Ther. Clin. Risk Manag.* **2007**, *3* (1), 71−97.

(8) Pappas, P. G.; Kauffman, C. A.; Andes, D. R.; Clancy, C. J.; Marr, K. A.; Ostrosky-Zeichner, L.; Reboli, A. C.; Schuster, M. G.; Vazquez, J. A.; Walsh, T. J.; Zaoutis, T. E.; Sobel, J. D. Executive Summary: Clinical Practice Guideline for the Management of Candidiasis: 2016 Update by the Infectious Diseases Society of America. *Clin. Infect. Dis.* **2016**, *62* (4), 409−417.

(9) Brown, G. D.; Denning, D. W.; Gow, N. A. R.; Levitz, S. M.; Netea, M. G.; White, T. C. Hidden Killers: Human Fungal Infections. *Sci. Transl. Med.* **2012**, *4*, No. 165rv13.

(10) Park, B. J.; Wannemuehler, K. A.; Marston, B. J.; Govender, N.; Pappas, P. G.; Chiller, T. M. Estimation of the Current Global Burden of Cryptococcal Meningitis among Persons Living with HIV/AIDS. *AIDS* **2009**, *23* (4), 525−530.

(11) Lepak, A. J.; Zhao, M.; VanScoy, B.; Ambrose, P. G.; Andes, D. R. Pharmacodynamics of a Long-Acting Echinocandin, CD101, in a Neutropenic Invasive-Candidiasis Murine Model Using an Extended-Interval Dosing Design. *Antimicrob. Agents Chemother.* **2018**, *62* (2). DOI: 10.1128/AAC.02154-17.

(12) Sofjan, A. K.; Mitchell, A.; Shah, D. N.; Nguyen, T.; Sim, M.; Trojcak, A.; Beyda, N. D.; Garey, K. W. Rezafungin (CD101), a next-Generation Echinocandin: A Systematic Literature Review and Assessment of Possible Place in Therapy. *J. Glob. Antimicrob. Resist.* **2018**, *14*, 58−64.

(13) Aimanianda, V.; Latgé, J.-P. Problems and Hopes in the Development of Drugs Targeting the Fungal Cell Wall. *Expert Rev. Anti-Infect. Ther.* **2010**, *8* (4), 359−364.

(14) Douglas, C. M.; D'Ippolito, J. A.; Shei, G. J.; Meinz, M.; Onishi, J.; Marrinan, J. A.; Li, W.; Abruzzo, G. K.; Flattery, A.; Bartizal, K.; Mitchell, A.; Kurtz, M. B. Identification of the *FKS1* Gene of *Candida albicans* as the Essential Target of 1,3-β-D-Glucan Synthase Inhibitors. *Antimicrob. Agents Chemother.* **1997**, *41* (11), 2471−2479.

(15) Douglas, C. M. Fungal β(1,3)-D-Glucan Synthesis. *Med. Mycol.* **2001**, *39*, 55−66.

(16) Chhetri, A.; Loksztejn, A.; Nguyen, H.; Pianalto, K. M.; Kim, M. J.; Hong, J.; Alspaugh, J. A.; Yokoyama, K. Length Specificity and Polymerization Mechanism of (1,3)-β- d -Glucan Synthase in Fungal Cell Wall Biosynthesis. *Biochemistry* **2020**, *59* (5), 682−693.

(17) Douglas, C. M.; Marrinan, J. A.; Li, W.; Kurtz, M. B. A *Saccharomyces cerevisiae* Mutant with Echinocandin-Resistant 1,3-β-D-Glucan Synthase. *J. Bacteriol.* **1994**, *176* (18), 5686−5696.

(18) Qadota, H.; Python, C. P.; Inoue, S. B.; Arisawa, M.; Anraku, Y.; Zheng, Y.; Watanabe, T.; Levin, D. E.; Ohya, Y. Identification of Yeast Rho1 p GTPase as a Regulatory Subunit of 1,3-β-Glucan Synthase. *Science* **1996**, *272* (5259), 279−281.

(19) Douglas, C. M.; Foor, F.; Marrinan, J. A.; Morin, N.; Nielsen, J. B.; Dahl, A. M.; Mazur, P.; Baginsky, W.; Li, W.; El-Sherbeini, M. The *Saccharomyces cerevisiae FKS1* (*ETG1*) Gene Encodes an Integral Membrane Protein Which Is a Subunit of 1,3-,8-D-Glucan Synthase. *Proc. Natl. Acad. Sci. U. S. A.* **1994**, *91*, 12907−12911.

(20) Okada, H.; Abe, M.; Asakawa-Minemura, M.; Hirata, A.; Qadota, H.; Morishita, K.; Ohnuki, S.; Nogami, S.; Ohya, Y. Multiple Functional Domains of the Yeast l,3-β-Glucan Synthase Subunit Fks1p Revealed by Quantitative Phenotypic Analysis of Temperature-Sensitive Mutants. *Genetics* **2010**, *184* (4), 1013−1024.

(21) Johnson, M. E.; Katiyar, S. K.; Edlind, T. D. New Fks Hot Spot for Acquired Echinocandin Resistance in *Saccharomyces cerevisiae* and Its Contribution to Intrinsic Resistance of Scedosporium Species. *Antimicrob. Agents Chemother.* **2011**, *55* (8), 3774−3781.

(22) Park, S.; Kelly, R.; Kahn, J. N.; Robles, J.; Hsu, M. J.; Register, E.; Li, W.; Vyas, V.; Fan, H.; Abruzzo, G.; Flattery, A.; Gill, C.; Chrebet, G.; Parent, S. A.; Kurtz, M.; Teppler, H.; Douglas, C. M.; Perlin, D. S. Specific Substitutions in the Echinocandin Target Fks1p Account for Reduced Susceptibility of Rare Laboratory and Clinical *Candida* Sp. Isolates. *Antimicrob. Agents Chemother.* **2005**, *49* (8), 3264−3273.

(23) Berman, J.; Krysan, D. J. Drug Resistance and Tolerance in Fungi. *Nat. Rev. Microbiol.* **2020**, *18* (6), 319−331.

(24) Johnson, M. E.; Edlind, T. D. Topological and Mutational Analysis of *Saccharomyces cerevisiae* Fks1. *Eukaryotic Cell* **2012**, *11* (7), 952−960.

(25) Healey, K. R.; Katiyar, S. K.; Raj, S.; Edlind, T. D. CRS-MIS in *Candida glabrata:* Sphingolipids Modulate Echinocandin-Fks Interaction. *Mol. Microbiol.* **2012**, *86* (2), 303−313.

(26) Paderu, P.; Park, S.; Perlin, D. S. Caspofungin Uptake Is Mediated by a High-Affinity Transporter in *Candida albicans*. *Antimicrob. Agents Chemother.* **2004**, *48* (10), 3845−3849.

(27) Pratt, A.; Garcia-Effron, G.; Zhao, Y.; Park, S.; Mustaev, A.; Pillai, S.; Perlin, D. S. Evaluation of Fungal-Specific Fluorescent Labeled Echinocandin Probes as Diagnostic Adjuncts. *Med. Mycol.* **2013**, *51* (1), 103−107.

(28) Huang, W.; Liao, G.; Baker, G. M.; Wang, Y.; Lau, R.; Paderu, P.; Perlin, D. S.; Xue, C. Lipid Flippase Subunit Cdc50 Mediates Drug

Resistance and Virulence in *Cryptococcus neoformans*. *mBio* **2016**, *7* (3). DOI: 10.1128/mBio.00478-16.
(29) Pfaller, M.; Boyken, L.; Hollis, R.; Kroeger, J.; Messer, S.; Tendolkar, S.; Diekema, D. Use of Epidemiological Cutoff Values to Examine 9-Year Trends in Susceptibility of *Candida* Species to Anidulafungin, Caspofungin, and Micafungin. *J. Clin. Microbiol.* **2011**, *49* (2), 624−629.
(30) Beyda, N. D.; Lewis, R. E.; Garey, K. W. Echinocandin Resistance in *Candida* Species: Mechanisms of Reduced Susceptibility and Therapeutic Approaches. *Ann. Pharmacother.* **2012**, *46* (7−8), 1086−1096.
(31) Dannaoui, E.; Desnos-Ollivier, M.; Garcia-Hermoso, D.; Grenouillet, F.; Cassaing, S.; Baixench, M. T.; Bretagne, S.; Dromer, F.; Lortholary, O. *Candida* Spp. with Acquired Echinocandin Resistance, France, 2004−2010. *Emerging Infect. Dis.* **2012**, *18* (1), 86−90.
(32) Maubon, D.; Garnaud, C.; Calandra, T.; Sanglard, D.; Cornet, M. Resistance of *Candida* Spp. to Antifungal Drugs in the ICU: Where Are We Now? *Intensive Care Med.* **2014**, *40*, 1241−1255.
(33) Felton, T.; Troke, P. F.; Hope, W. W. Tissue Penetration of Antifungal Agents. *Clinical Microbiology Reviews. Clin. Microbiol. Rev.* **2014**, *27* (1), 68−88.
(34) Zhao, Y.; Prideaux, B.; Nagasaki, Y.; Lee, M. H.; Chen, P. Y.; Blanc, L.; Ho, H.; Clancy, C. J.; Nguyen, M. H.; Dartois, V.; Perlin, D. S. Unraveling Drug Penetration of Echinocandin Antifungals at the Site of Infection in an Intra-Abdominal Abscess Model. *Antimicrob. Agents Chemother.* **2017**, *61* (10). DOI: 10.1128/AAC.01009-17.
(35) Stephens, D. J.; Allan, V. J. Light Microscopy Techniques for Live Cell Imaging. *Science* **2003**, *300*, 82−86.
(36) Zhang, J.; Campbell, R. E.; Ting, A. Y.; Tsien, R. Y. Creating New Fluorescent Probes for Cell Biology. *Nat. Rev. Mol. Cell Biol.* **2002**, *3*, 906−918, DOI: 10.1038/nrm976.
(37) Jaber, Q. Z.; Benhamou, R. I.; Herzog, I. M.; Ben Baruch, B.; Fridman, M. Cationic Amphiphiles Induce Macromolecule Denaturation and Organelle Decomposition in Pathogenic Yeast. *Angew. Chem., Int. Ed.* **2018**, *57* (50), 16391−16395.
(38) Benhamou, R. I.; Jaber, Q. Z.; Herzog, I. M.; Roichman, Y.; Fridman, M. Fluorescent Tracking of the Endoplasmic Reticulum in Live Pathogenic Fungal Cells. *ACS Chem. Biol.* **2018**, *13* (12), 3325−3332.
(39) Louzoun-Zada, S.; Jaber, Q. Z.; Fridman, M. Guiding Drugs to Target-Harboring Organelles: Stretching Drug-Delivery to a Higher Level of Resolution. *Angew. Chem., Int. Ed.* **2019**, *58*, 15584−15594.
(40) Benhamou, R. I.; Bibi, M.; Steinbuch, K. B.; Engel, H.; Levin, M.; Roichman, Y.; Berman, J.; Fridman, M. Real-Time Imaging of the Azole Class of Antifungal Drugs in Live *Candida* Cells. *ACS Chem. Biol.* **2017**, *12* (7), 1769−1777.
(41) Fery-Forgues, S.; Fayet, J. P.; Lopez, A. Drastic Changes in the Fluorescence Properties of NBD Probes with the Polarity of the Medium: Involvement of a TICT State? *J. Photochem. Photobiol., A* **1993**, *70* (3), 229−243.
(42) Geisow, M. J. Fluorescein Conjugates as Indicators of Subcellular PH. A Critical Evaluation. *Exp. Cell Res.* **1984**, *150* (1), 29−35.
(43) Yang, L.; Simionescu, R.; Lough, A.; Yan, H. Some Observations Relating to the Stability of the BODIPY Fluorophore under Acidic and Basic Conditions. *Dyes Pigm.* **2011**, *91* (2), 264−267.
(44) Pfaller, M. A.; Diekema, D. J.; Ostrosky-Zeichner, L.; Rex, J. H.; Alexander, B. D.; Andes, D.; Brown, S. D.; Chaturvedi, V.; Ghannoum, M. A.; Knapp, C. C.; Sheehan, D. J.; Walsh, T. J. Correlation of MIC with Outcome for *Candida* Species Tested against Caspofungin, Anidulafungin, and Micafungin: Analysis and Proposal for Interpretive MIC Breakpoints. *J. Clin. Microbiol.* **2008**, *46* (8), 2620−2629.
(45) Richards, A.; Gow, N. A. R.; Veses, V. Identification of Vacuole Defects in Fungi. *J. Microbiol. Methods* **2012**, *91* (1), 155−163.
(46) Stefan, C. J.; Blumer, K. J. A Syntaxin Homolog Encoded by VAM3Mediates Down-Regulation of a Yeast G Protein-Coupled Receptor. *J. Biol. Chem.* **1999**, *274* (3), 1835−1841.
(47) Johnston, D. A.; Eberle, K. E.; Sturtevant, J. E.; Palmer, G. E. Role for Endosomal and Vacuolar GTPases in *Candida albicans* Pathogenesis. *Infect. Immun.* **2009**, *77* (6), 2343−2355.
(48) Vida, T. A.; Emr, S. D. A New Vital Stain for Visualizing Vacuolar Membrane Dynamics and Endocytosis in Yeast. *J. Cell Biol.* **1995**, *128* (5), 779−792.
(49) Schmid, S. L.; Carter, L. L. ATP Is Required for Receptor-Mediated Endocytosis in Intact Cells. *J. Cell Biol.* **1990**, *111*, 2307−2318.
(50) Feinberg, A. P.; Snyder, S. H. Phenothiazine Drugs: Structure Activity Relationships Explained by a Conformation That Mimics Dopamine. *Proc. Natl. Acad. Sci. U. S. A.* **1975**, *72* (5), 1899−1903.
(51) Neale, R. F.; Fallon, S. L.; Boyar, W. C.; Wasley, J. W. F.; Martin, L. L.; Stone, G. A.; Glaeser, B. S.; Sinton, C. M.; Williams, M. Biochemical and Pharmacological Characterization of CGS 12066B, a Selective Serotonin-1B Agonist. *Eur. J. Pharmacol.* **1987**, *136* (1), 1−9.
(52) Bar-Yosef, H.; Vivanco Gonzalez, N.; Ben-Aroya, S.; Kron, S. J.; Kornitzer, D. Chemical Inhibitors of *Candida albicans* Hyphal Morphogenesis Target Endocytosis. *Sci. Rep.* **2017**, *7* (1), 1−12.
(53) Moreno-Velásquez, S. D.; Seidel, C.; Juvvadi, P. R.; Steinbach, W. J.; Read, N. D. Caspofungin-Mediated Growth Inhibition and Paradoxical Growth in *Aspergillus fumigatus* Involve Fungicidal Hyphal Tip Lysis Coupled with Regenerative Intrahyphal Growth and Dynamic Changes in β-1,3-Glucan Synthase Localization. *Antimicrob. Agents Chemother.* **2017**, *61* (10), No. e00710.
(54) Ben-Ami, R.; Garcia-Effron, G.; Lewis, R. E.; Gamarra, S.; Leventakos, K.; Perlin, D. S.; Kontoyiannis, D. P. Fitness and Virulence Costs of *Candida albicans FKS1* Hot Spot Mutations Associated with Echinocandin Resistance. *J. Infect. Dis.* **2011**, *204* (4), 626−635.
(55) Garcia-Effron, G.; Lee, S.; Park, S.; Cleary, J. D.; Perlin, D. S. Effect of *Candida glabrata FKS1* and *FKS2* Mutations on Echinocandin Sensitivity and Kinetics of 1,3-β-D-Glucan Synthase: Implication for the Existing Susceptibility Breakpoint. *Antimicrob. Agents Chemother.* **2009**, *53* (9), 3690−3699.
(56) Carreté, L.; Ksiezopolska, E.; Pegueroles, C.; Gómez-Molero, E.; Saus, E.; Iraola-Guzmán, S.; Loska, D.; Bader, O.; Fairhead, C.; Gabaldón, T. Patterns of Genomic Variation in the Opportunistic Pathogen *Candida glabrata* Suggest the Existence of Mating and a Secondary Association with Humans. *Curr. Biol.* **2018**, *28* (1), 15.
(57) Ene, I. V.; Walker, L. A.; Schiavone, M.; Lee, K. K.; Martin-Yken, H.; Dague, E.; Gow, N. A. R.; Munro, C. A.; Brown, A. J. P. Cell Wall Remodeling Enzymes Modulate Fungal Cell Wall Elasticity and Osmotic Stress Resistance. *mBio* **2015**, *6* (4). DOI: 10.1128/mBio.00986-15.
(58) Schwarzmüller, T.; Ma, B.; Hiller, E.; Istel, F.; Tscherner, M.; Brunke, S.; Ames, L.; Firon, A.; Green, B.; Cabral, V.; Marcet-Houben, M.; Jacobsen, I. D.; Quintin, J.; Seider, K.; Frohner, I.; Glaser, W.; Jungwirth, H.; Bachellier-Bassi, S.; Chauvel, M.; Zeidler, U.; Ferrandon, D.; Gabaldón, T.; Hube, B.; d'Enfert, C.; Rupp, S.; Cormack, B.; Haynes, K.; Kuchler, K. Systematic Phenotyping of a Large-Scale *Candida glabrata* Deletion Collection Reveals Novel Antifungal Tolerance Genes. *PLoS Pathog.* **2014**, *10* (6), No. e1004211.
(59) Walker, L. A.; Gow, N. A. R.; Munro, C. A. Fungal Echinocandin Resistance. *Fungal Genet. Biol.* **2010**, *47* (2), 117−126.
(60) Stevens, D. A.; Espiritu, M.; Parmar, R. Paradoxical Effect of Caspofungin: Reduced Activity against *Candida albicans* at High Drug Concentrations. *Antimicrob. Agents Chemother.* **2004**, *48* (9), 3407−3411.
(61) Cota, J. M.; Grabinski, J. L.; Talbert, R. L.; Burgess, D. S.; Rogers, P. D.; Edlind, T. D.; Wiederhold, N. P. Increases in SLT2 Expression and Chitin Content Are Associated with Incomplete Killing of *Candida glabrata* by Caspofungin. *Antimicrob. Agents Chemother.* **2008**, *52* (3), 1144−1146.

(62) Imtiaz, T.; Lee, K. K.; Munro, C. A.; MacCallum, D. M.; Shankland, G. S.; Johnson, E. M.; MacGregor, M. S.; Bal, A. M. Echinocandin Resistance Due to Simultaneous FKS Mutation and Increased Cell Wall Chitin in a *Candida albicans* Bloodstream Isolate Following Brief Exposure to Caspofungin. *J. Med. Microbiol.* **2012**, *61* (9), 1330−1334.
(63) Hoch, H. C.; Galvani, C. D.; Szarowski, D. H.; Turner, J. N. Two New Fluorescent Dyes Applicable for Visualization of Fungal Cell Walls. *Mycologia* **2005**, *97* (3), 580−588.
(64) Lee, K. K.; MacCallum, D. M.; Jacobsen, M. D.; Walker, L. A.; Odds, F. C.; Gow, N. A. R.; Munro, C. A. Elevated Cell Wall Chitin in *Candida albicans* Confers Echinocandin Resistance in Vivo. *Antimicrob. Agents Chemother.* **2012**, *56* (1), 208−217.
(65) Walker, L. A.; Gow, N. A. R.; Munro, C. A. Elevated Chitin Content Reduces the Susceptibility of *Candida* Species to Caspofungin. *Antimicrob. Agents Chemother.* **2013**, *57* (1), 146−154.
(66) De Groot, P. W. J.; Kraneveld, E. A.; Yin, Q. Y.; Dekker, H. L.; Groß, U.; Crielaard, W.; De Koster, C. G.; Bader, O.; Klis, F. M.; Weig, M. The Cell Wall of the Human Pathogen *Candida glabrata*: Differential Incorporation of Novel Adhesin-like Wall Proteins. *Eukaryotic Cell* **2008**, *7* (11), 1951−1964.
(67) Proctor, S. A.; Minc, N.; Boudaoud, A.; Chang, F. Contributions of Turgor Pressure, the Contractile Ring, and Septum Assembly to Forces in Cytokinesis in Fission Yeast. *Curr. Biol.* **2012**, *22* (17), 1601−1608.
(68) Speers, A. E.; Cravatt, B. F. Profiling Enzyme Activities in Vivo Using Click Chemistry Methods. *Chem. Biol.* **2004**, *11* (4), 535−546.
(69) Lampkins, A. J.; O'Neil, E. J.; Smith, B. D. Bio-Orthogonal Phosphatidylserine Conjugates for Delivery and Imaging Applications. *J. Org. Chem.* **2008**, *73* (16), 6053−6058.

https://dx.doi.org/10.1021/acscentsci.0c00813
ACS Cent. Sci. 2020, 6, 1698−1712